

Global/Regional Non-hydrostatic Numerical Weather Prediction Model Using Semi-implicit and Semi-Lagrangian Method

~progress and challenge ~

Xueshun Shen
Center for Numerical Prediction
China Meteorological Administration



Outline

- Background & overview of CMA NWP
- Introduction of GRAPES model
 - Continuous equations
 - Temporal discretization
 - Spatial discretization
 - Solution procedure
- Future development



Current major operational NWP systems

	Global Spectral Model (T _L 639L60)	Meso Scale Model (GRAPES_Meso)	10day Ensemble (T213L31)	Typhoon deterministic & Ensemble forecast
Forecast range	Medium-range (10day)	Rainfall forecast Short-range forecast	10day forecast	Typhoon forecast
Forecast domain	Global	East Asia (8340km x 5480km)	Global	
Horizontal resolution	T _L 639(0.28125 deg)	15km	T213(0.5625 deg)	
Vertical levels / Top	60 0.1 hPa	31 10hPa	31 10 hPa	
Forecast Hours (Initial time)	240 hours (00, 12 UTC) 84 hours (06, 18UTC)	72 hours (00, 12UTC)	240 hours (00, 12 UTC) 15 members	120 hours (00, 06, 12, 18 UTC) 120 hours (00, 12 UTC) 15 members
Initial Condition	Global Analysis (NCEP GSI)	GRAPES_3DVAR	NCEP SSI + Vortex relocation and Intensity adjustment with ensemble perturbations Perturbations are produced by Breeding-method	

About GRAPES

GRAPES (Global/Regional Assimilation PrEiction System), project launched since 2001.

What GRAPES main features are?

A unified NWP system

- *A unified dynamic core* with different configurations of physics for different applications
- 3/4-VAR data assimilation



CMA's GRAPES Model

It's a single model for :

- Operational **weather** forecasts at
 - Mesoscale (GRAPES_Meso: grid-size \sim 15km \rightarrow 3km)
 - Global scale (GRAPES_GFS: grid size \sim 50km)
 - + **Research** mode (grid size \sim 1km \rightarrow 20m) & LES、single column model
- 13 years old since its development to 2013



Governing equations

Fully compressible with shallow atmospheric approximation

Spherical & Z coordinate

Prognostic variables:

u : east-west wind

v : north-south wind

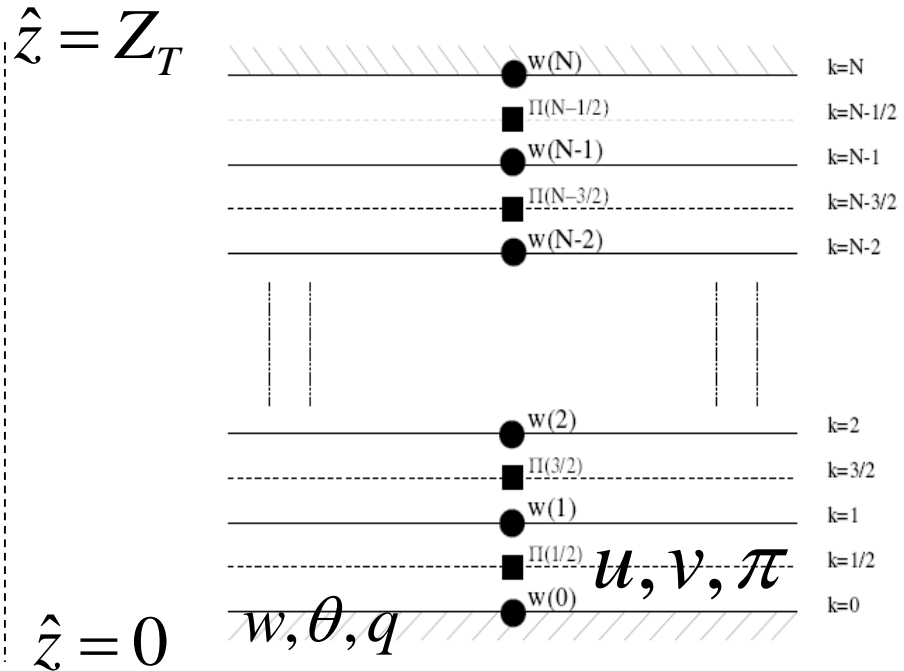
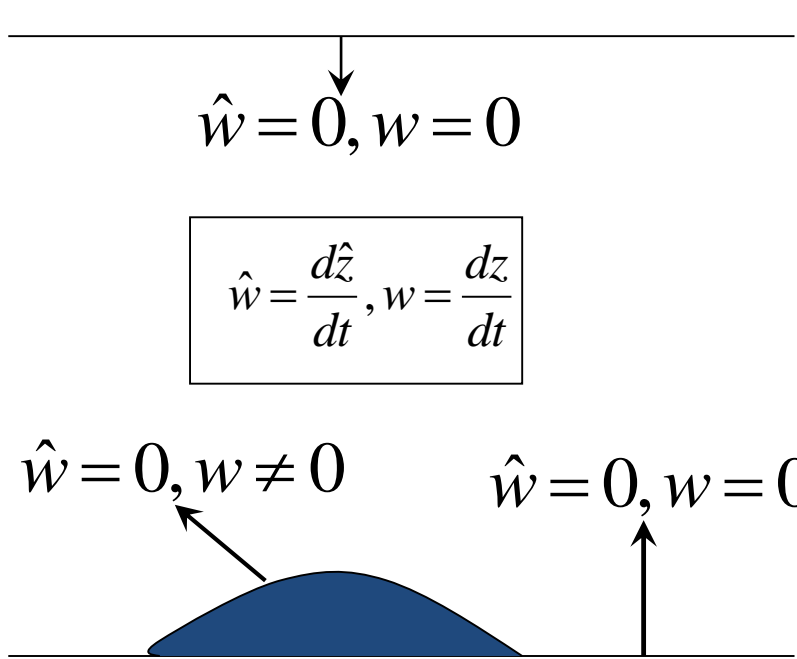
θ : potential temperature

π : pressure, Exner function

m_x : mixing ratio of tracers

$$\left\{
 \begin{aligned}
 \frac{du}{dt} &= -\frac{C_p \theta_v}{r \cos \varphi} \frac{\partial \Pi}{\partial \lambda} + fv + F_u + \delta_M \left\{ \frac{u \cdot v \cdot \tan \varphi}{r} - \frac{u \cdot w}{r} \right\} - \delta_\varphi \{ f_\varphi w \} \\
 \frac{dv}{dt} &= -\frac{C_p \theta_v}{r} \frac{\partial \Pi}{\partial \varphi} - fu + F_v - \delta_M \left\{ \frac{u^2 \cdot \tan \varphi}{r} + \frac{v \cdot w}{r} \right\} \\
 \delta_{NH} \frac{dw}{dt} &= -C_p \theta_v \frac{\partial \Pi}{\partial r} - g + F_w + \delta_M \left\{ \frac{u^2 + v^2}{r} \right\} + \delta_\varphi \{ f_\varphi u \} \\
 (\gamma - 1) \frac{d\Pi}{dt} &= -\Pi \cdot D_3 + \frac{F_\theta^*}{\theta_v} \\
 \frac{d\theta}{dt} &= \frac{F_\theta^*}{\Pi} \\
 \frac{dm_x}{dt} &= Sm_x \\
 p &= \rho R_d T_v
 \end{aligned}
 \right.$$

Boundary conditions

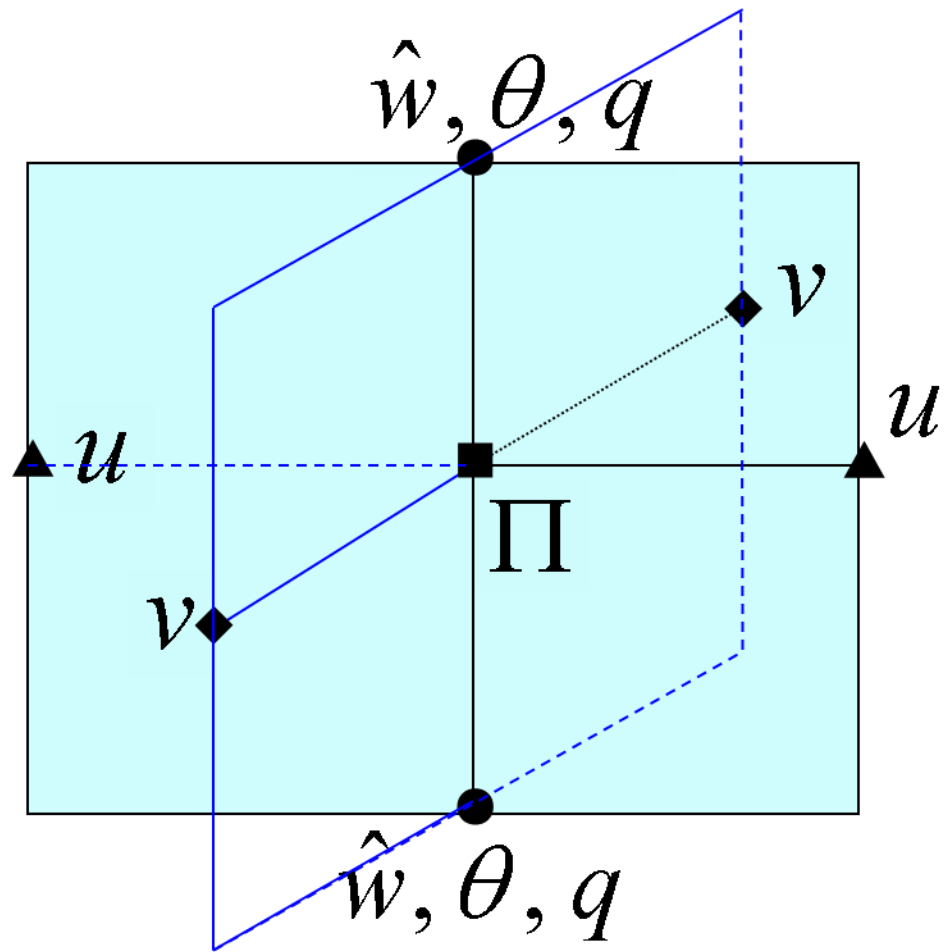
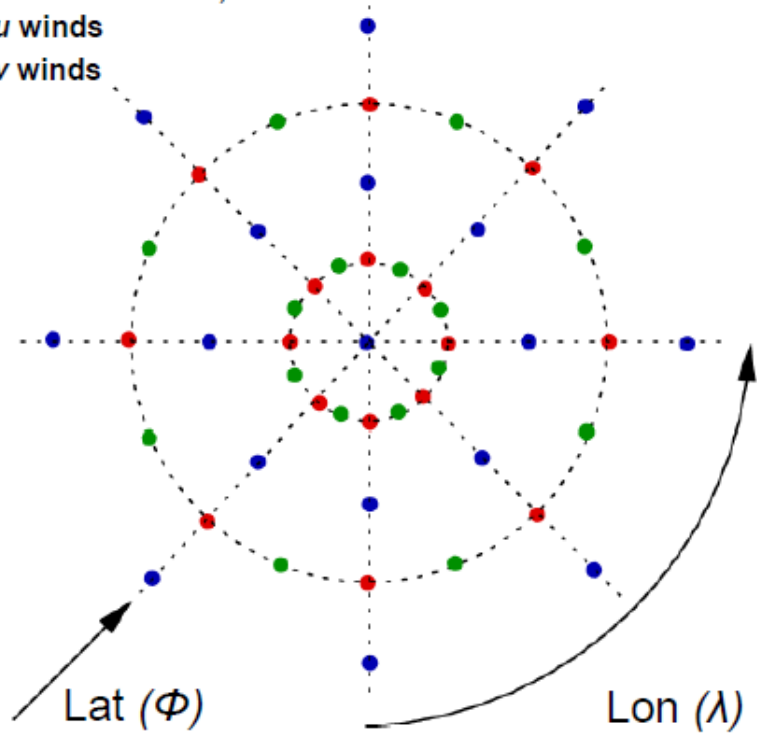


For the regional model (Davies, 1976)

$$\bar{F}_l^{n+1} = \alpha_l \cdot F_{LS} + (1 - \alpha_l) \cdot F_l^{n+1}$$

Grid structure

- Scalar variables, w winds
- ● u winds
- v winds



Modified Arakawa-C in the horizontal
V-point at poles

Charney-Phillips vertical grid

Temporal discretization

Off-centered two-time level semi-implicit semi-Lagrangian scheme

Why off-centered 2TL SISL?

- Two-time level scheme is more efficient than three-time level scheme
- Off centered:
 - To address spurious SL orographic resonance (Rivest et al., 1994)
 - To provide required damping to keep the scheme stable
- Semi-implicit:
 - To treat all terms involving the fastest propagation speeds implicitly (acoustic waves, gravity waves)
 - To allow the longer time step
 - To improve the scheme stability



Semi-Lagrangian scalar advection

- The governing equations of scalar variables can be written generically as (linearized using a stationary reference profile):

$$\frac{D\psi}{Dt} = L(x, t, \psi) + N(x, t, \psi)$$

- Integrate along Lagrangian trajectory

$$\begin{aligned}\int_t^{t+\Delta t} \frac{D\psi}{Dt} dt &= \frac{\psi^{t+\Delta t}(x) - \psi^t(x - U\Delta t)}{\Delta t} = \int_t^{t+\Delta t} (L(x, t, \psi) + N(x, t, \psi)) dt \\ &\approx (1-\alpha)(L+N)_{D(x-U\Delta t)}^t + \alpha(L+N)_A^{t+\Delta t} \quad \text{↗ } \alpha : \text{offcentering coefficient} \\ \underline{\underline{(\psi - \alpha\Delta t(L+N))_A^{t+\Delta t}}} &= \underline{\underline{(\psi + (1-\alpha)\Delta t(L+N))_D^t}}\end{aligned}$$



Temporal discretization formula for scalar variables

$$(\theta')_A^{t+\Delta t} = \Delta t \alpha (L_\theta)_A^{t+\Delta t} + (A_\theta)_D^t$$

$$(\Pi')_A^{t+\Delta t} = \Delta t \alpha (L_\Pi)_A^{t+\Delta t} + (A_\Pi)_D^t$$



Scalar advection for conserved variables

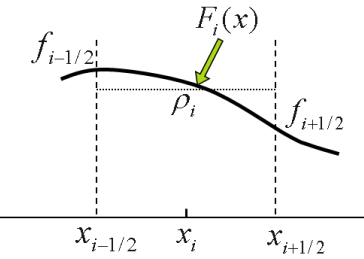
- Semi-Lagrangian schemes allow
 - Enhanced stability, longer time-step (no CFL limit)
 - Accurate handling of meteorologically important slow modes
- But, point-wise interpolation → **non-conservation**, e.g., moisture etc.
- In GRAPES, **a conservative semi-Lagrangian scheme based on local reconstruction using rational function**



Scalar advection schemes for conserved variables

- PRM (Piece-wise rational method): conservative semi-Lagrangian scheme with positive-definite, higher accuracy

**Single cell reconstruction based on
cell-integrated average and interface value: PRM**



PRM (Conservative Semi-Lagrangian) reconstruction:

- ◆ $f_{i+1/2}$ independent of the cell-integrated average, solved through a semi-Lagrangian solution
- ◆ More accurate numerical dispersion
- ◆ A global continuous reconstruction
- ◆ Much easier to suppress numerical oscillation

A semi-Lagrangian approach for the interface value

$$\begin{cases} \tilde{f}(x_{i+1/2}, t + \Delta t) = F(x_{i+1/2} - \xi_{i+1/2}, t) \\ f(x_{i+1/2}, t) = \tilde{f}(x_{i+1/2}, t) - \int_{\bar{\tau}} f \frac{\partial u}{\partial x} d\tau \end{cases}$$

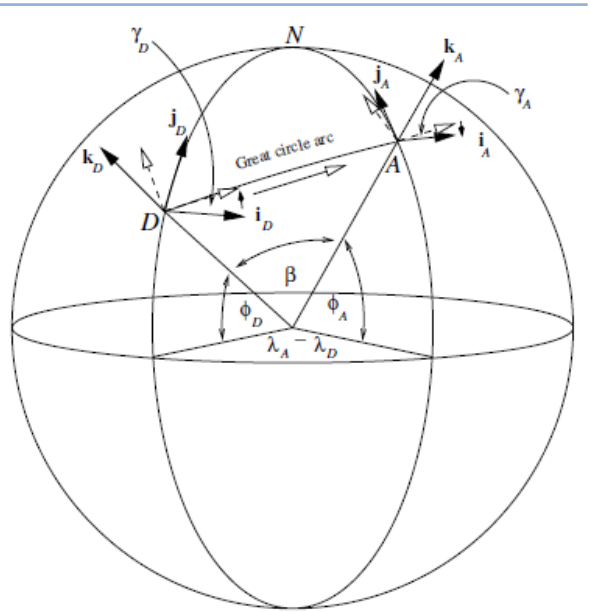
$\bar{\tau}$: trajectory between $(x_{i+1/2} - \xi_{i+1/2}, t)$ and $(x_{i+1/2}, t + \Delta t)$

Semi-Lagrangian advection for momentum equations (vector) in curved geometry

$$\frac{D\vec{u}}{Dt} = L(x, t, \vec{u}) + N(x, t, \vec{u}) = \vec{\phi}$$

Integrate along trajectory

$$\vec{u}_A(x_A^{t+\Delta t}, t + \Delta t) = \vec{u}_D(x_D^t, t) + [\alpha \vec{\varphi}_A(x_A^{t+\Delta t}, t + \Delta t) + (1 - \alpha) \vec{\varphi}_D(x_D^t, t)] \Delta t$$



Consider changes of unit vectors at A and D

$$\begin{pmatrix} u_A \\ v_A \\ w_A \end{pmatrix} = \mathbf{M} \begin{pmatrix} u_D \\ v_D \\ w_D \end{pmatrix} + (1 - \alpha) \Delta t \begin{pmatrix} \varphi_D^x \\ \varphi_D^y \\ \varphi_D^z \end{pmatrix} + \alpha \Delta t \begin{pmatrix} \varphi_A^x \\ \varphi_A^y \\ \varphi_A^z \end{pmatrix}$$

\mathbf{M} : rotation matrix

$$\begin{pmatrix} i_A \cdot i_D & i_A \cdot j_D & i_A \cdot k_D \\ j_A \cdot i_D & j_A \cdot j_D & j_A \cdot k_D \\ k_A \cdot i_D & k_A \cdot j_D & k_A \cdot k_D \end{pmatrix}$$

Temporal discretization formula for vector variables

$$u_A^{t+\Delta t} = \Delta t \alpha_\varepsilon (L_u)_A^{t+\Delta t} + (A_u)_D^t$$

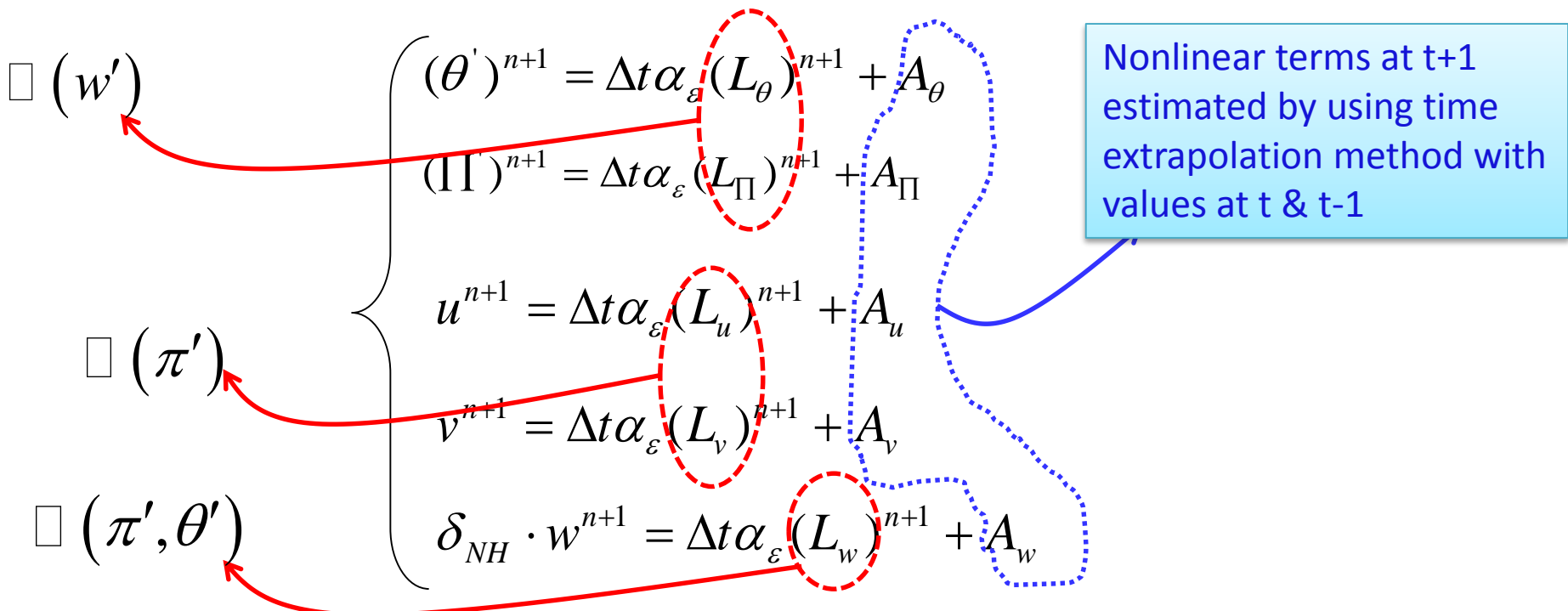
$$v_A^{t+\Delta t} = \Delta t \alpha_\varepsilon (L_v)_A^{t+\Delta t} + (A_v)_D^t$$

$$\delta_{NH} \cdot w_A^{t+\Delta t} = \Delta t \alpha_\varepsilon (L_w)_A^{t+\Delta t} + (A_w)_D^t$$

The similar formulation of temporal discretization as scalar prognostic variables, but with the **position factors**



Summary: prognostic equations after temporal discretization



Further algebraic manipulation

$$\left\{ \begin{array}{l} u = (\xi_{u1} \frac{1}{a \cos \varphi} \frac{\partial}{\partial \lambda} + \xi_{u2} \frac{1}{a} \frac{\partial}{\partial \varphi} + \xi_{u3} \frac{\partial}{\partial \hat{z}}) \Pi' + \xi_{u0} \\ v = (\xi_{v1} \frac{1}{a \cos \varphi} \frac{\partial}{\partial \lambda} + \xi_{v2} \frac{1}{a} \frac{\partial}{\partial \varphi} + \xi_{v3} \frac{\partial}{\partial \hat{z}}) \Pi' + \xi_{v0} \\ \hat{w} = [\xi_{w1} \frac{1}{a \cos \varphi} \frac{\partial}{\partial \lambda} + \xi_{w2} \frac{1}{a} \frac{\partial}{\partial \varphi} + \xi_{w3} \frac{\partial}{\partial \hat{z}}] \Pi' + \xi_{w0} \\ \theta' = [\xi_{\theta1} \frac{1}{a \cos \varphi} \frac{\partial}{\partial \lambda} + \xi_{\theta2} \frac{1}{a} \frac{\partial}{\partial \varphi} + \xi_{\theta3} \frac{\partial}{\partial \hat{z}}] \Pi' + \xi_{\theta0} \\ \Pi' = \xi_{\Pi1} \cdot u + \xi_{\Pi2} \cdot v + \xi_{\Pi3} \cdot \hat{w} + \xi_{\Pi4} \cdot D_3|_{\hat{z}} + \xi_{\Pi0} \end{array} \right.$$

So, $u^{n+1}, v^{n+1}, \hat{w}^{n+1}, (\theta')^{n+1}$ can be expressed as the function of

$$(\Pi')^{n+1}$$

$$u = (\xi_{u1} \frac{1}{a \cos \varphi} \frac{\partial}{\partial \lambda} + \xi_{u2} \frac{1}{a} \frac{\partial}{\partial \varphi} + \xi_{u3} \frac{\partial}{\partial \hat{z}}) \Pi + \xi_{u0}$$

$$v = (\xi_{v1} \frac{1}{a \cos \varphi} \frac{\partial}{\partial \lambda} + \xi_{v2} \frac{1}{a} \frac{\partial}{\partial \varphi} + \xi_{v3} \frac{\partial}{\partial \hat{z}}) \Pi + \xi_{v0}$$

Spatial discretization

$$\bar{F}^\lambda = \frac{1}{2} [F(\lambda + \frac{\Delta \lambda}{2}) + F(\lambda - \frac{\Delta \lambda}{2})]$$

$$F_x = \frac{\partial F}{\partial x} = \frac{1}{\Delta x} [F(x + \frac{\Delta x}{2}) - F(x - \frac{\Delta x}{2})]$$

$$\hat{w} = [\xi_{w1} \frac{1}{a \cos \varphi} \frac{\partial}{\partial \lambda} + \xi_{w2} \frac{1}{a} \frac{\partial}{\partial \varphi} + \xi_{w3} \frac{\partial}{\partial \hat{z}}] \Pi + \xi_{w0}$$

$$\hat{\theta} = [\xi_{\theta1} \frac{1}{a \cos \varphi} \frac{\partial}{\partial \lambda} + \xi_{\theta2} \frac{1}{a} \frac{\partial}{\partial \varphi} + \xi_{\theta3} \frac{\partial}{\partial \hat{z}}] \Pi + \xi_{\theta0}$$

Second-order accurate finite-differencing

$$u = \xi_{u1} \Pi_\lambda + \xi_{u2} (\bar{\Pi}^{\phi\lambda})_\phi + \xi_{u3} (\bar{\Pi}^{\hat{z}\lambda})_{\hat{z}} + \xi_{u0}$$

$$v = \xi_{v1} (\bar{\Pi}^{\lambda\phi})_\lambda + \xi_{v2} \Pi_\phi + \xi_{v3} (\bar{\Pi}^{\hat{z}\phi})_{\hat{z}} + \xi_{v0}$$

$$\hat{w} = \xi_{w1} (\bar{\Pi}^{\hat{z}\lambda})_\lambda + \xi_{w2} (\bar{\Pi}^{\hat{z}\phi})_\phi + \xi_{w3} \Pi_{\hat{z}} + \xi_{w0}$$

$$\hat{\theta} = \xi_{\theta1} (\bar{\Pi}^{\hat{z}\lambda})_\lambda + \xi_{\theta2} (\bar{\Pi}^{\hat{z}\phi})_\phi + \xi_{\theta3} \Pi_{\hat{z}} + \xi_{\theta0}$$



Spatial discretization

(continued)

Substituting the above spatial discretized u, v, \hat{w}, θ equations into the following continuity equation:

$$\Pi' = \xi_{\Pi 1} \cdot u + \xi_{\Pi 2} \cdot v + \xi_{\Pi 3} \cdot \hat{w} + \xi_{\Pi 4} \cdot D_3|_{\hat{z}} + \xi_{\Pi 0}$$



$$\begin{aligned} \Pi' &= \xi_{\Pi 1} [\xi_{u1} \Pi_\lambda + \xi_{u2} (\bar{\Pi}^{\phi\lambda})_\phi + \xi_{u3} (\bar{\Pi}^{\hat{z}\lambda})_{\hat{z}}]^\lambda + \xi_{\Pi 2} [\xi_{v1} (\bar{\Pi}^{\lambda\phi})_\lambda + \xi_{v2} \Pi_\phi + \xi_{v3} (\bar{\Pi}^{\hat{z}\phi})_{\hat{z}}]^\phi \\ &\quad + \xi_{\Pi 3} \cdot \xi_{w3z} \frac{\partial \Pi'}{\partial \hat{z}} + \xi_{\Pi 4} \cdot \{ [\xi_{u1} \Pi_\lambda + \xi_{u2} (\bar{\Pi}^{\phi\lambda})_\phi + \xi_{u3} (\bar{\Pi}^{\hat{z}\lambda})_{\hat{z}}]_\lambda \\ &\quad + [\xi_{v1} (\bar{\Pi}^{\lambda\phi})_\lambda + \xi_{v2} \Pi_\phi + \xi_{v3} (\bar{\Pi}^{\hat{z}\phi})_{\hat{z}}]_\phi + [\xi_{w1} (\bar{\Pi}^{\hat{z}\lambda})_\lambda + \xi_{w2} (\bar{\Pi}^{\hat{z}\phi})_\phi + \xi_{w3} \Pi_{\hat{z}}]_{\hat{z}} \} + \xi_{\Pi 0} \end{aligned}$$



Spatial discretization

(continued)

After some algebraic operations:

Helmholtz equation about Π'

$$\begin{aligned} & B_1 \Pi_{i,j,k} + B_2 \Pi_{i-1,j,k} + B_3 \Pi_{i+1,j,k} + B_4 \Pi_{i,j-1,k} + B_5 \Pi_{i,j+1,k} \\ & + B_6 \Pi_{i+1,j+1,k} + B_7 \Pi_{i+1,j-1,k} + B_8 \Pi_{i-1,j-1,k} + B_9 \Pi_{i-1,j+1,k} + \\ & B_{10} \Pi_{i,j,k-1} + B_{11} \Pi_{i-1,j,k-1} + B_{12} \Pi_{i+1,j,k-1} + B_{13} \Pi_{i,j-1,k-1} + B_{14} \Pi_{i,j+1,k-1} \\ & + B_{15} \Pi_{i,j,k+1} + B_{16} \Pi_{i-1,j,k+1} + B_{17} \Pi_{i+1,j,k+1} + B_{18} \Pi_{i,j-1,k+1} + B_{19} \Pi_{i,j+1,k+1} \\ & = (\xi_{\Pi 0})_{i,j,k} \end{aligned}$$



GRAPES dynamical core is solved as

- (1) Solve the Helmholtz equation to obtain $(\Pi')^{n+1}$
- (2) Then, easily get $u^{n+1}, v^{n+1}, \hat{w}^{n+1}, (\theta')^{n+1}$

Helmholtz eq. is solved by using
Pre-conditioned General Conjugate Residual Method(GCR)



Trajectory calculation

By solving the kinematic equation:

$$\frac{d\vec{x}}{dt} = \vec{u}$$

Discretized trajectory equation and mid-point rule

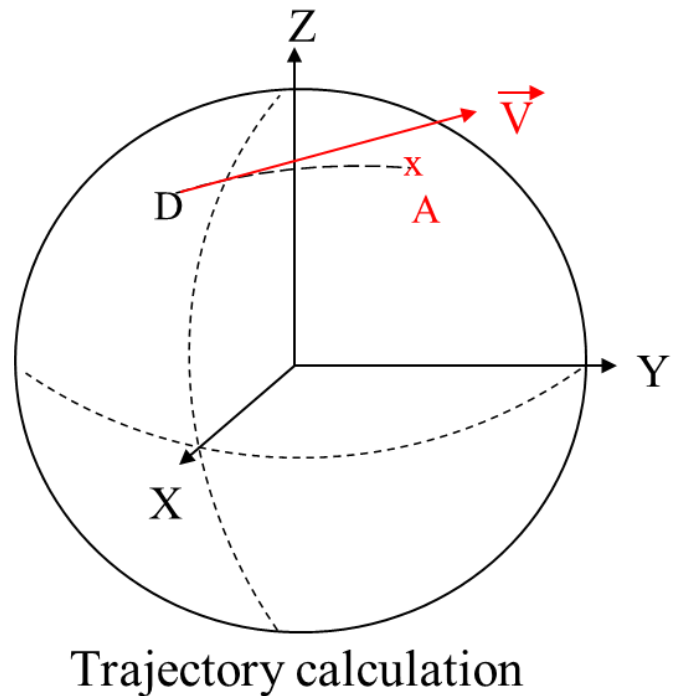
Iterate

$$x_a - x_d = \Delta t u\left(\frac{x_a + x_d}{2}, t^{n+\frac{1}{2}}\right)$$

$$x_d^{[l+1]} = x_a - \Delta t u\left(\frac{x_a + x_d^l}{2}, t^{n+\frac{1}{2}}\right), \quad l = 0, 1$$

Time extrapolation of winds

$$u^{n+\frac{1}{2}} = \frac{3}{2}u^n - \frac{1}{2}u^{n-1}$$



Spherical & polar effect in calculating trajectory

Ritche & Beaudoin (1994) method **within** ($80^\circ S - 80^\circ N$)

McDonald & Bates (1989) method **beyond** ($80^\circ S - 80^\circ N$)

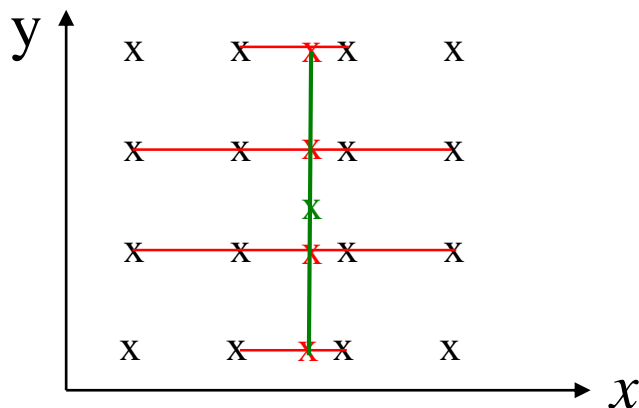
Interpolation method for obtaining the variables at departure point

GRAPES model uses
quasi-monotone quasi-cubic Lagrange interpolation

Cubic Lagrange interpolation:

$$\varphi(x) = \sum_{i=1}^4 C_i(x) \varphi_i \quad \text{with the weights}$$

$$C_i(x) = \frac{\prod_{k \neq i}^4 (x - x_k)}{\prod_{k \neq i}^4 (x_i - x_k)}$$

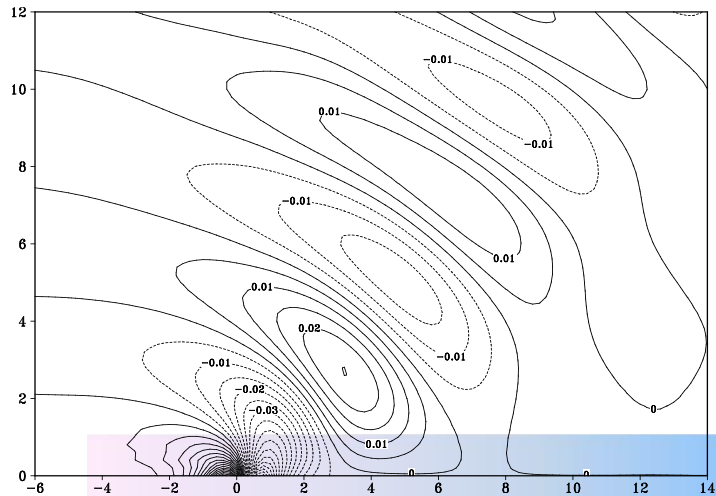


Idealized experiments

Dynamical core evaluation

2D test

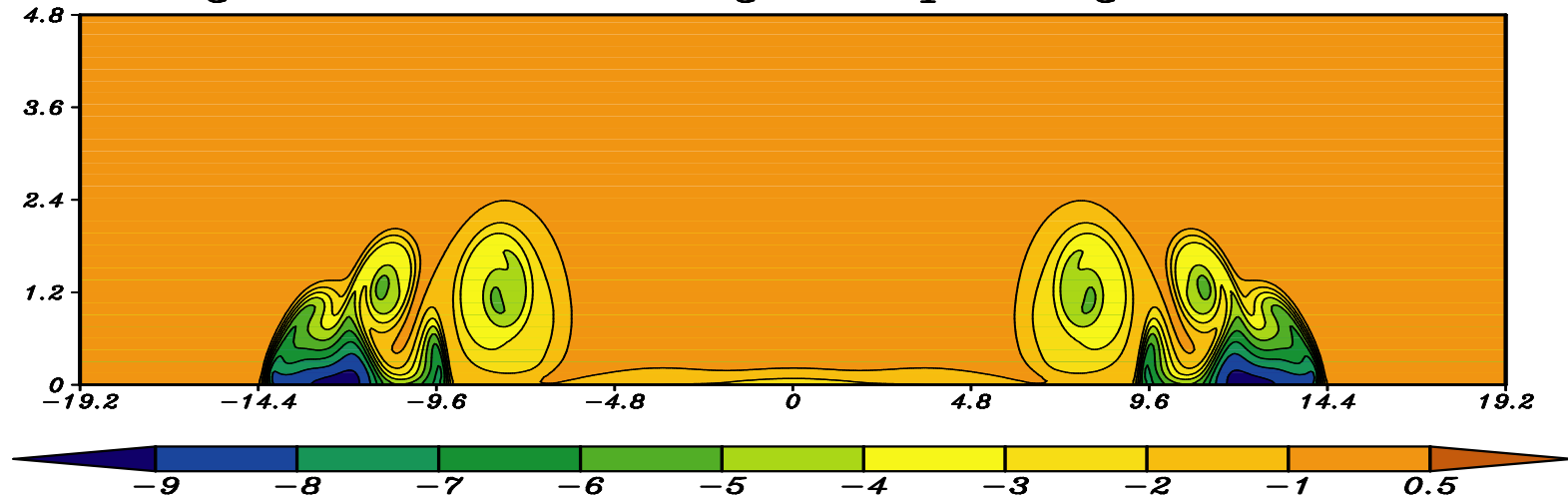
1. Density current
2. Warm bubble
3. Mountain wave



3D test

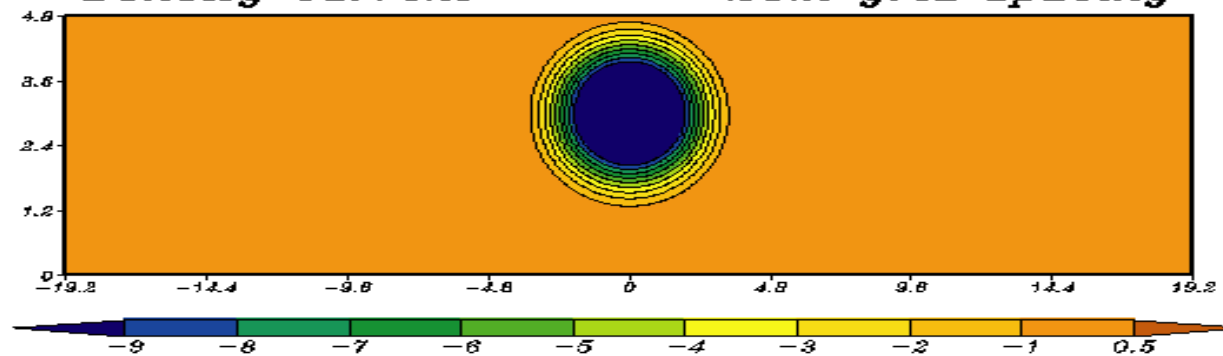
1. 3D tracer transport
2. Geostrophic balanced flow
3. Held & Suarez test
4. Rossby-Haurwitz wave
5. Mountain-induced Rossby wave
6. Mountain-induced Rossby wave with tracer
7. Baroclinic instability
8. Gravity and inertia-gravity waves
9. Cross-polar flow

Density current 25m grid spacing 900 seconds



Density current

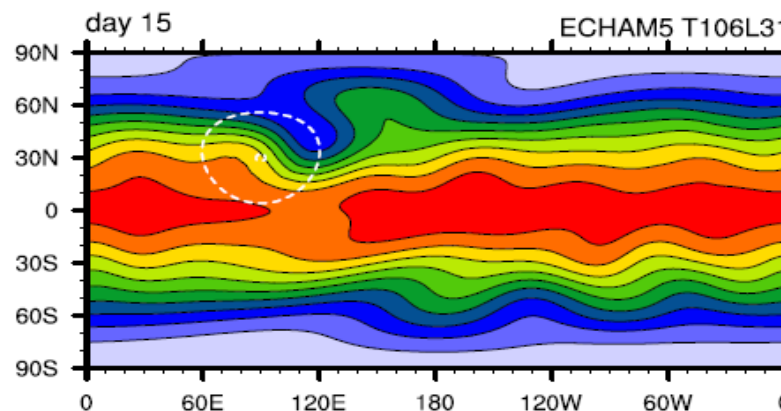
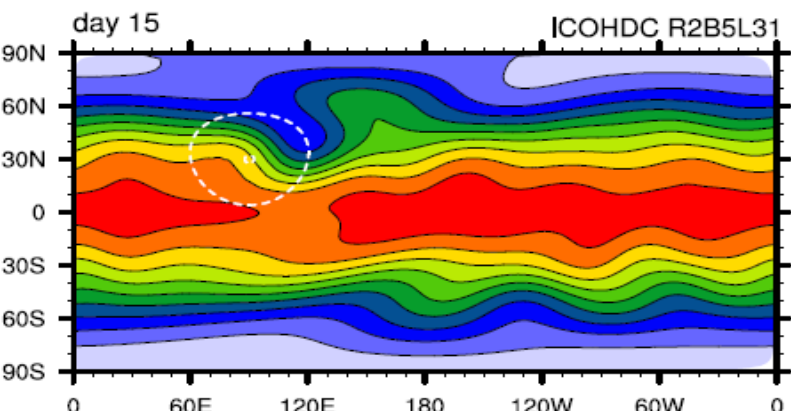
25m grid spacing



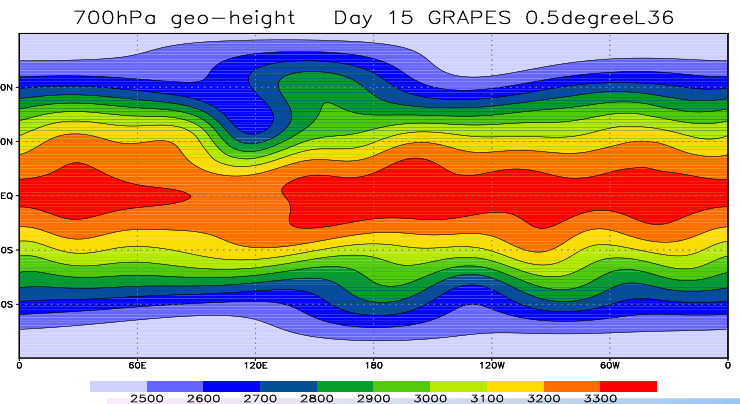
- Initial u , p_s , z_s fields, isothermal, $v=0$ m/s, balanced
- Mountain triggers the evolution of Rossby waves
- Hydrostatic, nonlinear regime

Mountain-induced Rossby wave

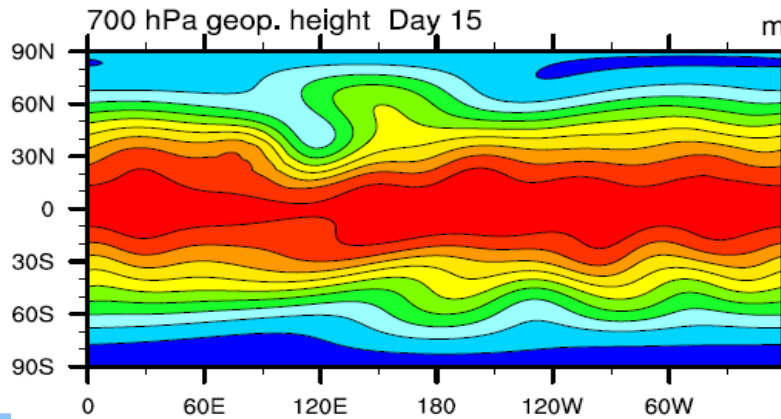
15day integration



GRAPES



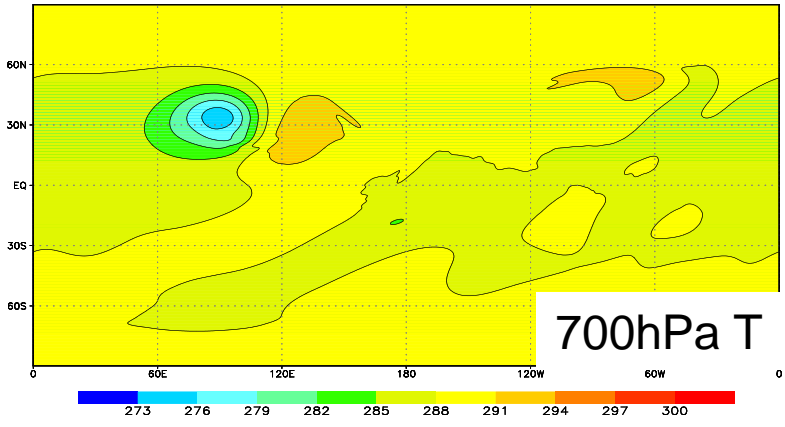
FV181*360L26



Courtesy: Dr. Jablonowski & Dr. H. Wan

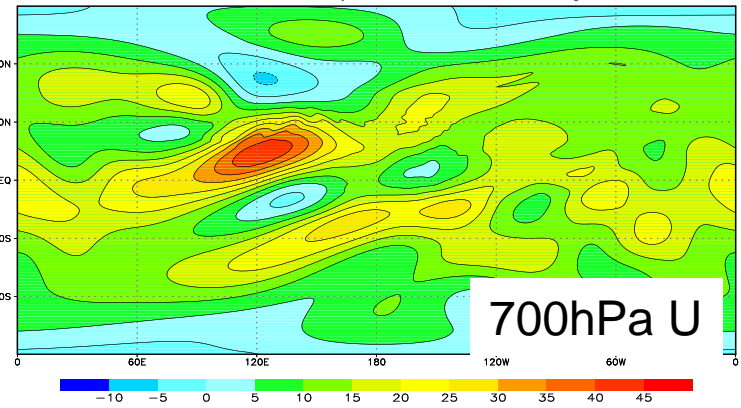


700hPa temperature Day 15 GRAPES 0.5degreeL36



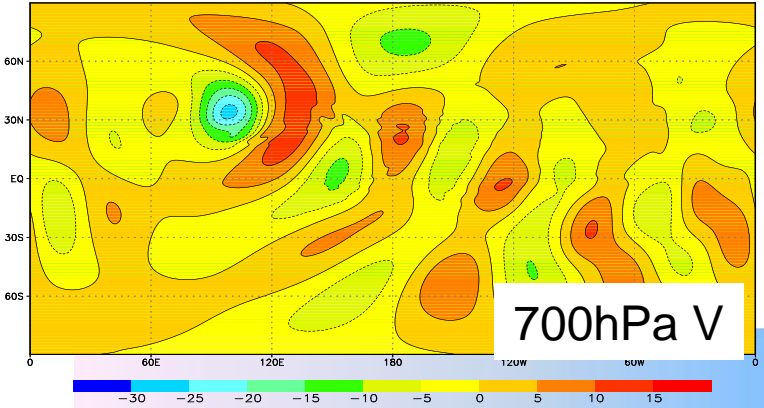
700hPa T

700hPa u-wind Day 15 GRAPES 0.5degreeL36



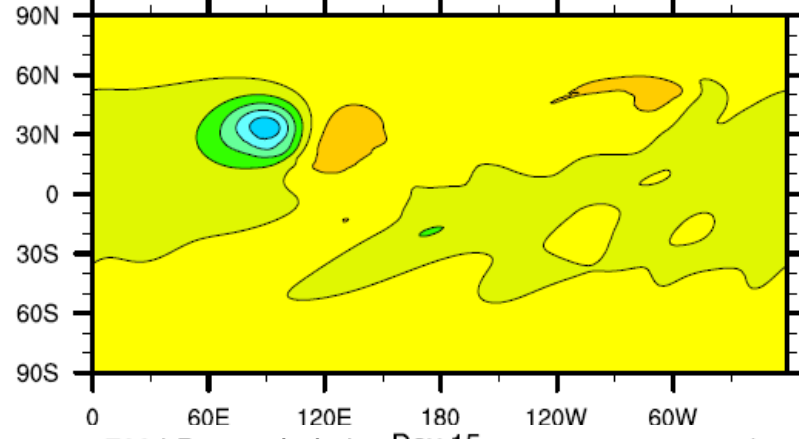
700hPa U

700hPa v-wind Day 15 GRAPES 0.5degreeL36



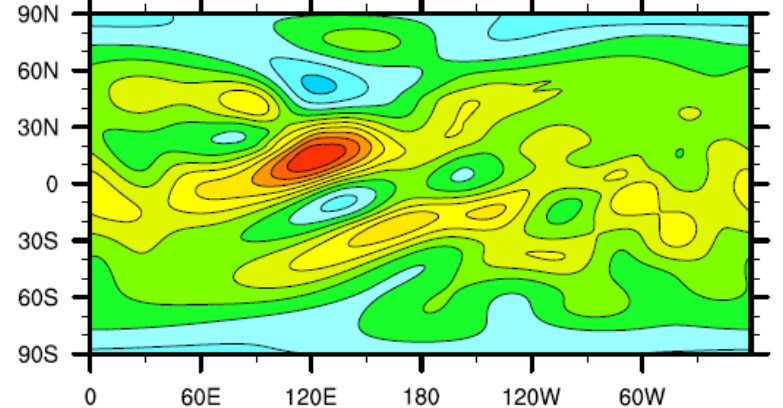
700hPa V

700 hPa temperature Day 15



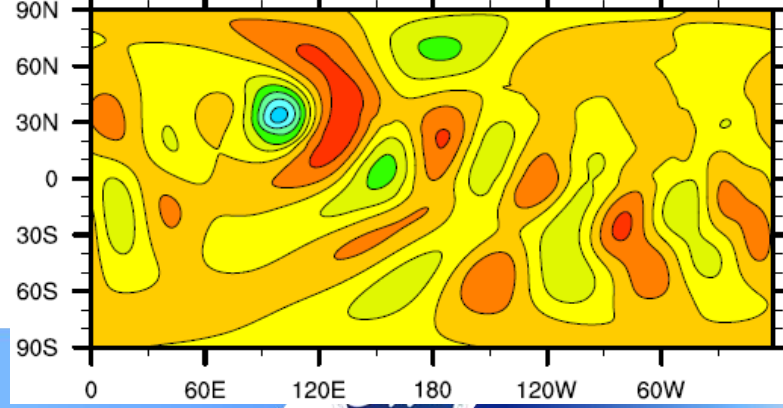
m/s

700 hPa zonal wind Day 15



NCAR FV

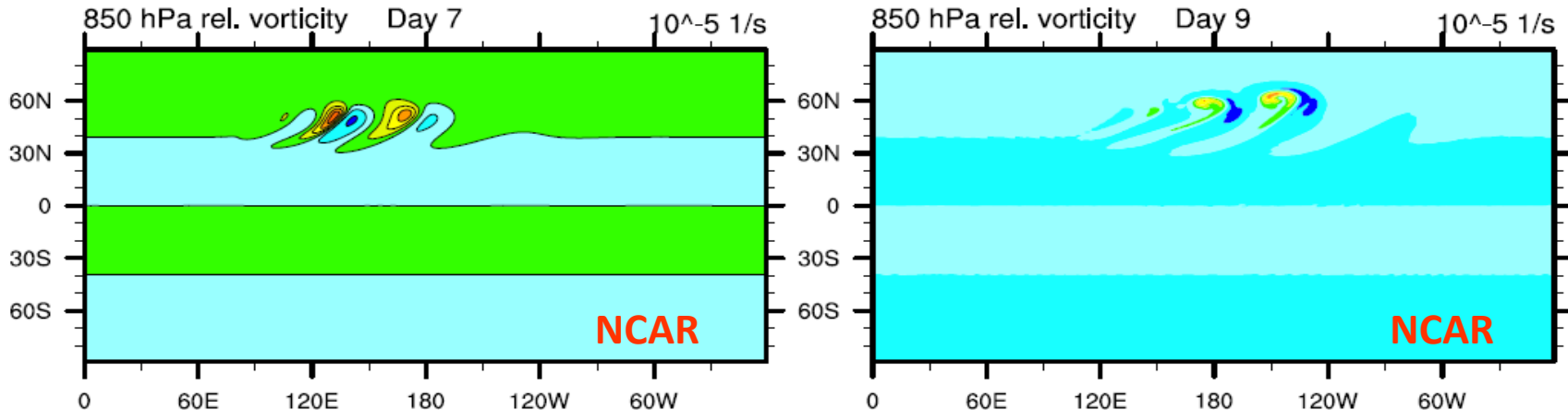
700 hPa merid. wjnd Day 15



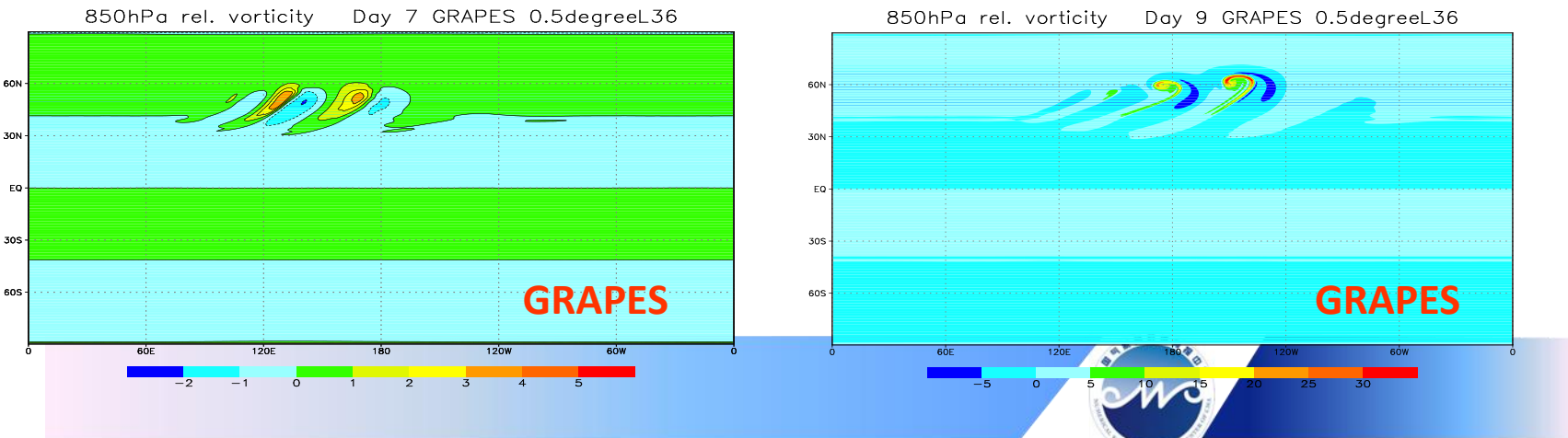
- A baroclinic wave can be triggered if the initial conditions for the steady-state are overlaid with a perturbation
- A perturbation with a Gaussian profile is selected and centered at (20°E, 40°N)

Baroclinic wave

(Jablonowski & Williamson, 2006)



Baroclinic wave growing, cyclone genesis & wave-train breaks



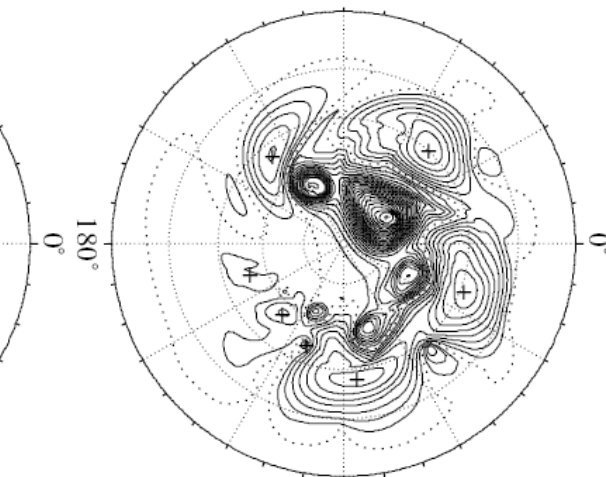
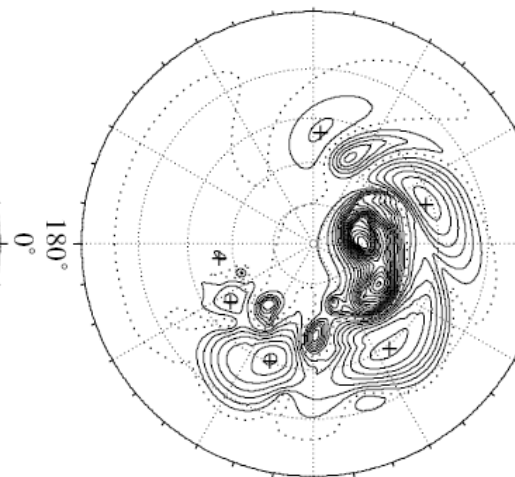
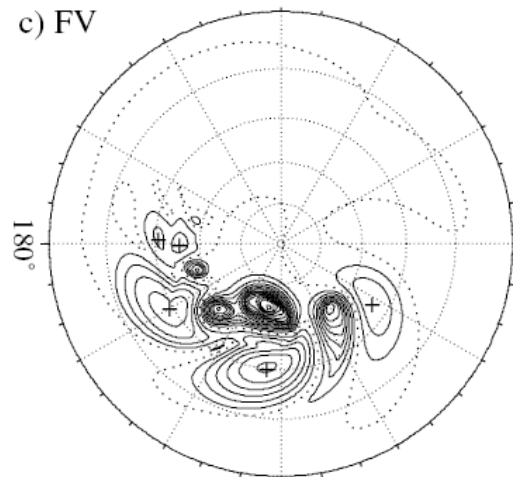
Surface pressure

Day 11

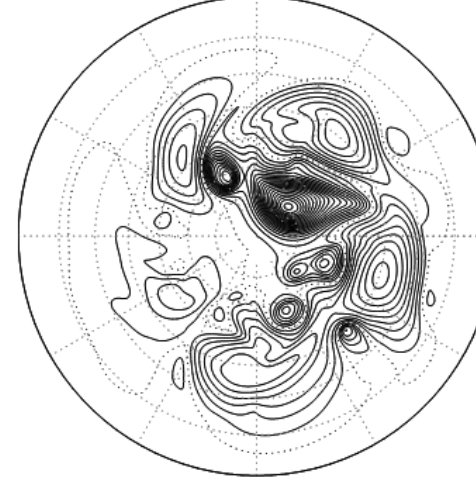
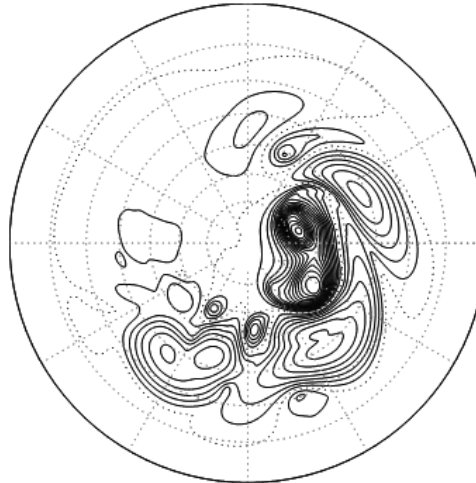
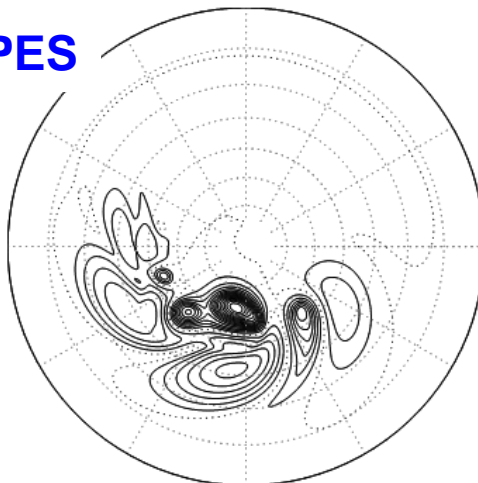
Day 14

Day 16

c) FV



GRAPES



(Jablonowski & Williamson, 2006)



Model physics package

- WRF physics for meso-scale application
- Physics
 - Radiation:
 - RRTMG LW(λ 4.71)/SW(λ 3.61)
 - Cumulus:
 - Simplified Arakawa Schubert
 - Microphysics: CMA two-moment microphysics with macro consideration
 - Cloud: Xu & Randall diagnostic cloud
 - Land surface: CoLM
 - Gravity wave drag:
 - Kim & Arakawa 1995; Lott & Miller 1997; Alpert, 2004
 - Small scale orographic form drag : Beljaars, Brown & Wood(2004)



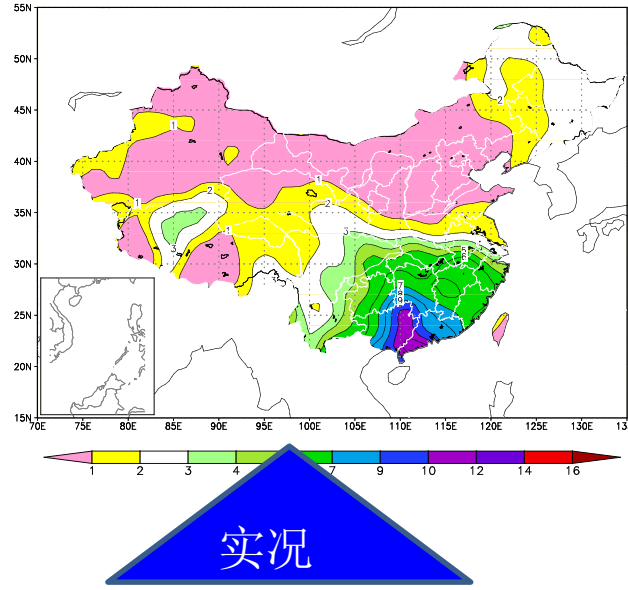
Current Applications of GRAPES

- **Global medium-range deterministic forecast**
 - GRAPES_GFS
- **Regional deterministic forecast**
 - GRAPES_Meso in NMC
 - GRAPES_TMM in GuangZhou
- **Typhoon track and intensity forecast**
 - GRAPES_TYM in NMC
 - GRAPES_TCM in Shanghai
- **Dust-storm forecast**
 - GRAPES_SDM

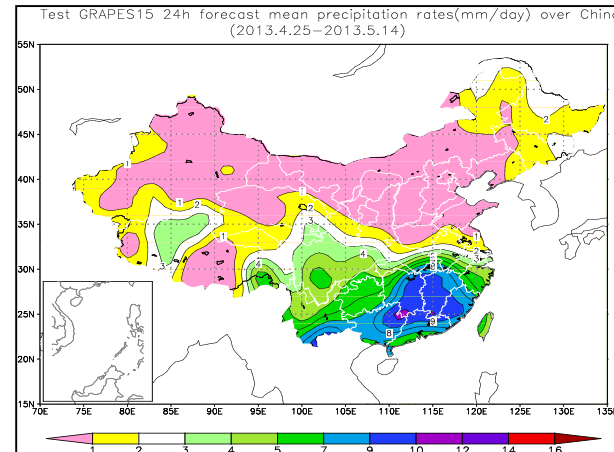


降水分布

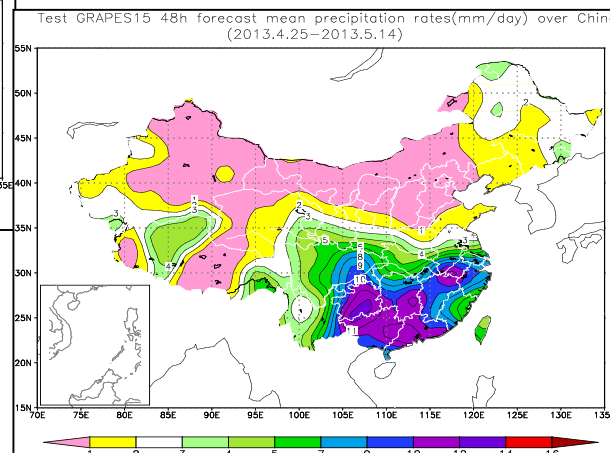
Mean precipitation rates(mm/day) over China(2013.4.25–2013.5.14)



24h

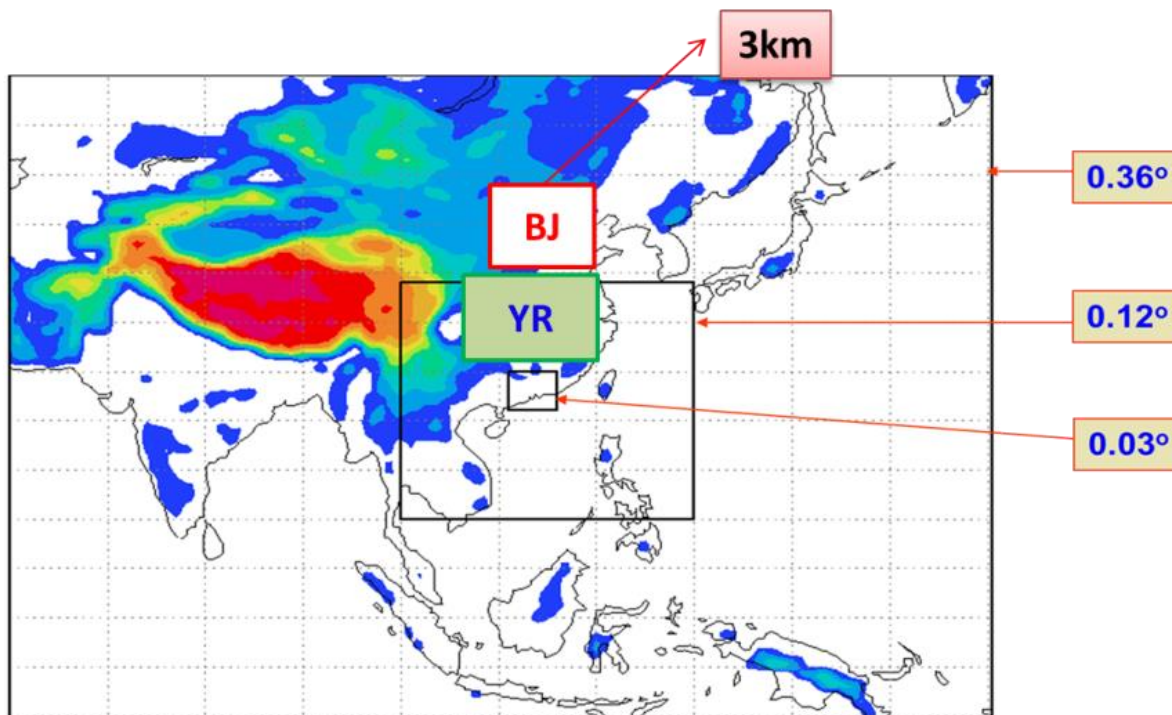


48h



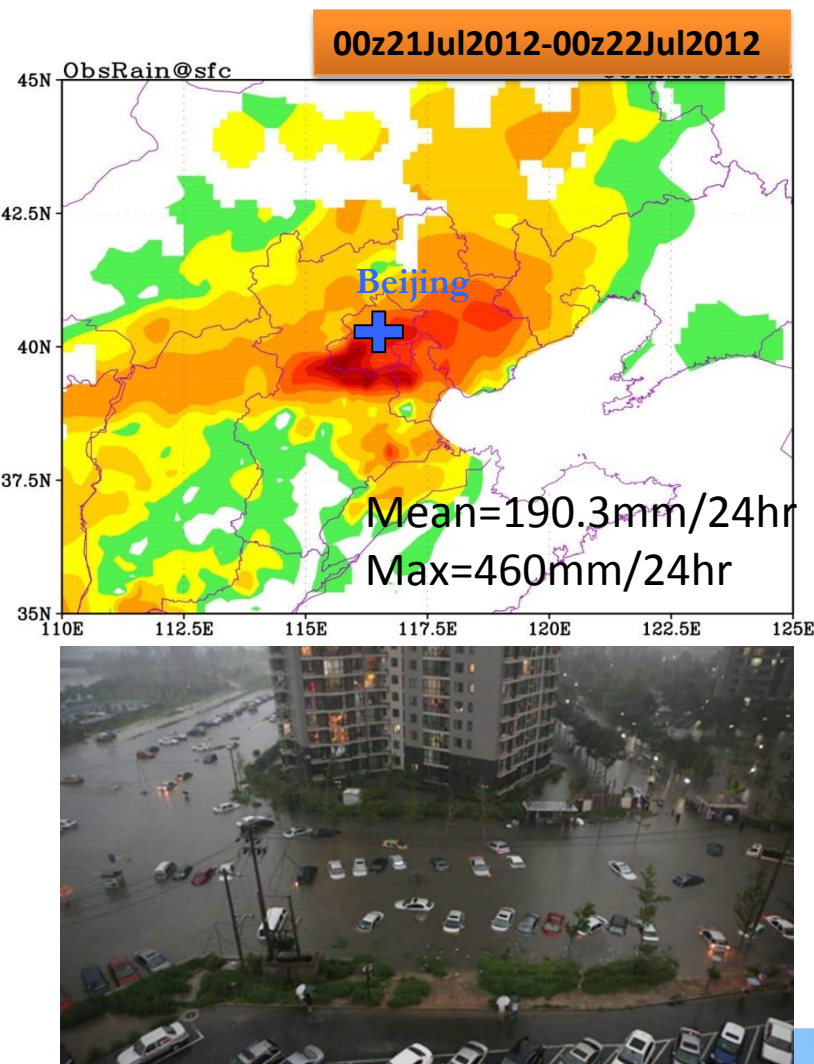
GRAPES 3~5km预报系统

高分辨率数值预报窗口



Heavy rainfall event on Jul.21/2012

Beijing



Initial: global analysis

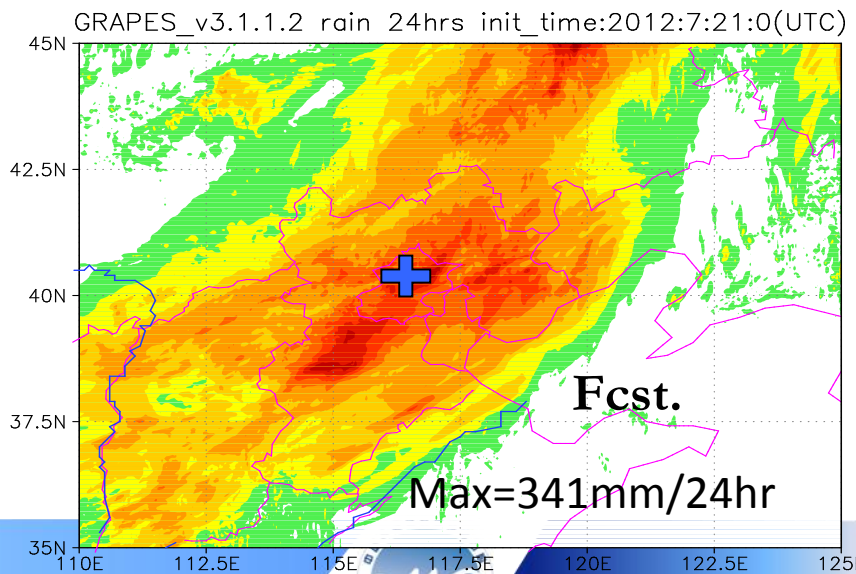
BC: global forecast

Grid size:3km

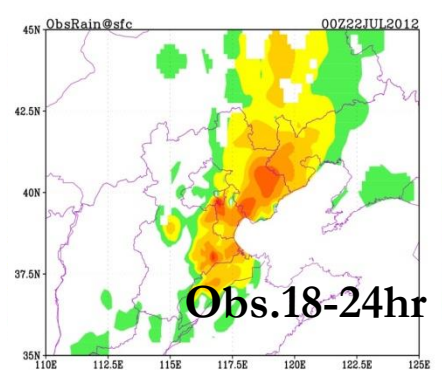
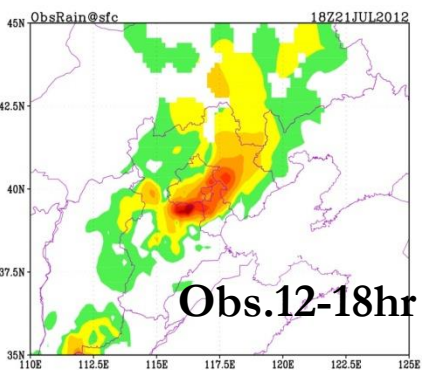
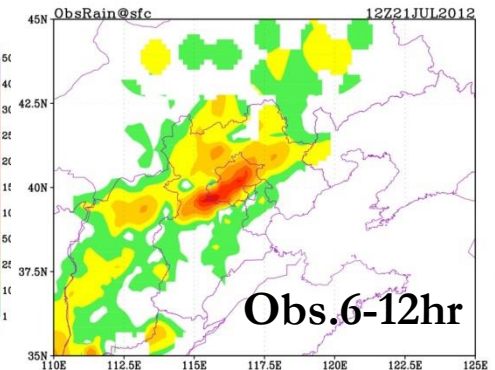
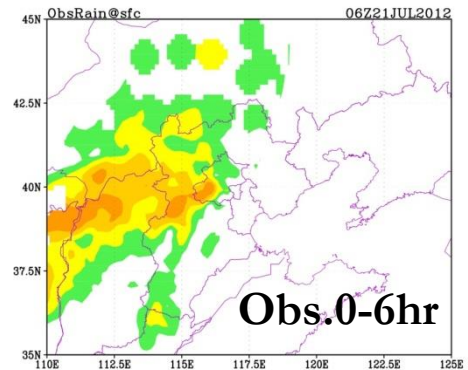
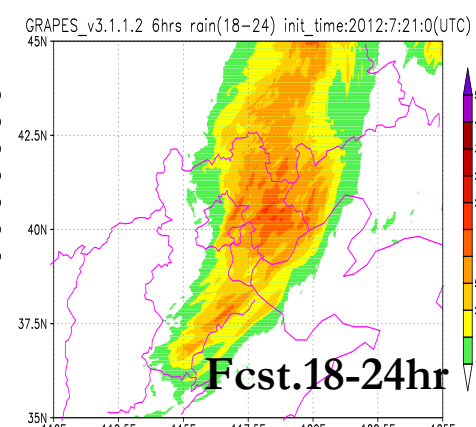
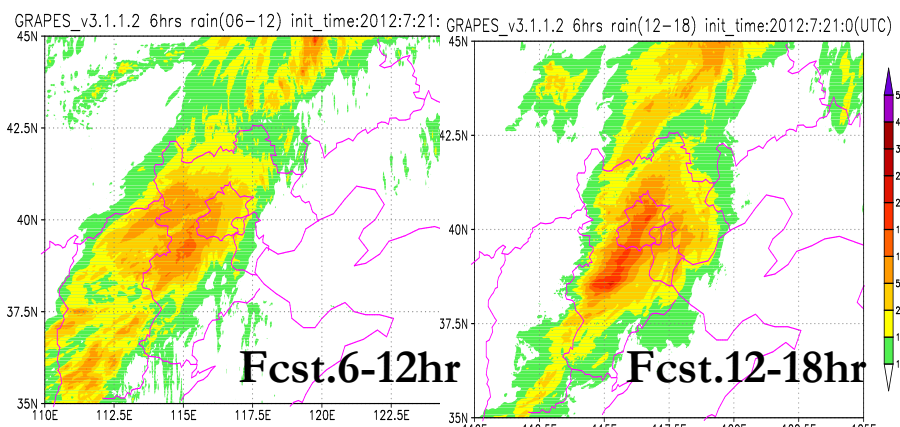
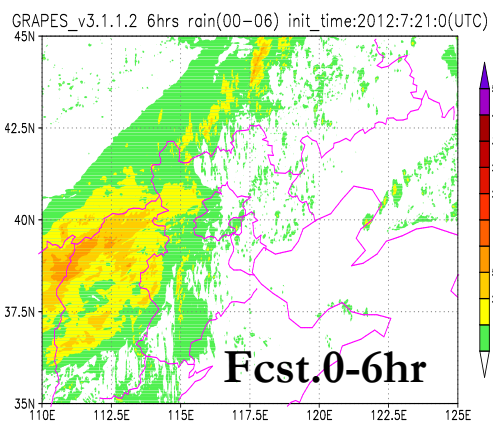
Physics:

- microphysics: WSM6
- radiation: RRTM S&L
- pbl : MRF
- land surface : NOAH

24-hour accumulated rainfall



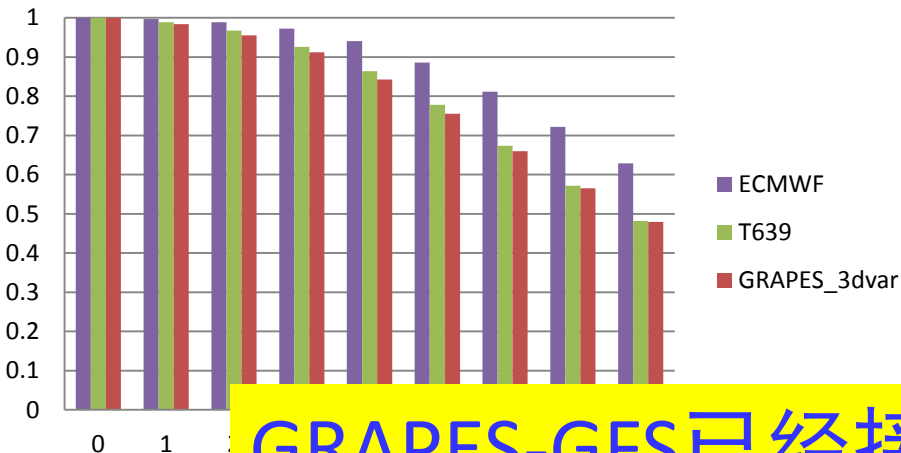
Comparison of precipitation every 6-hour between Obs. & Fcst.



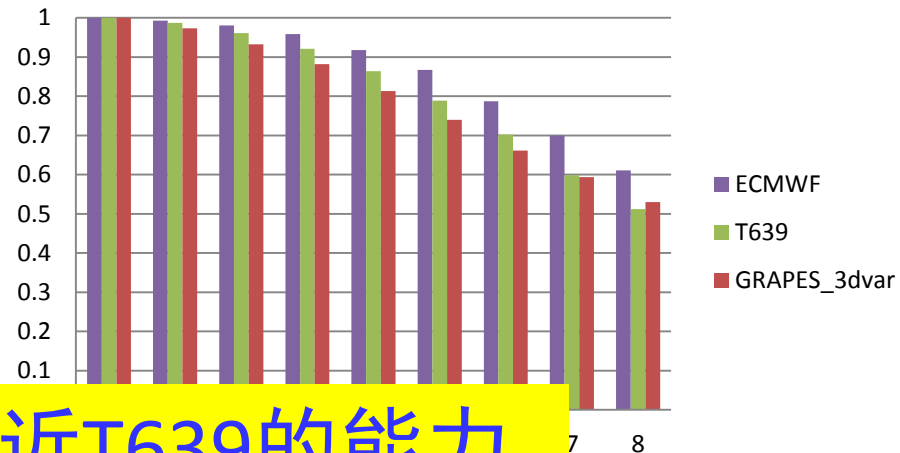
GRAPES全球预报系统

与ECMWF、T639的比较

北半球500hpa高度距平相关系数

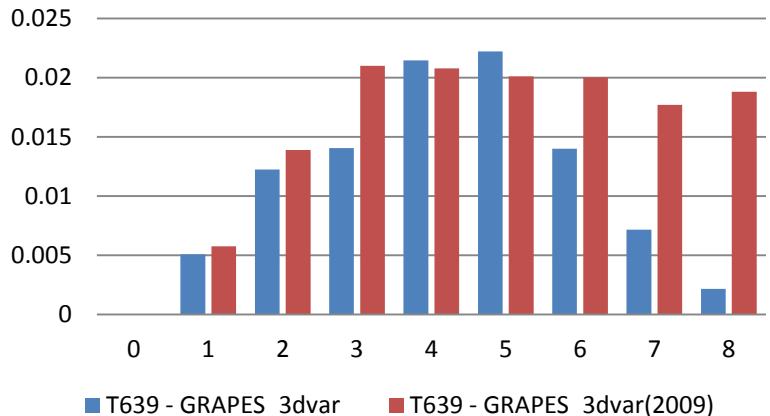


东亚500hpa高度距平相关系数

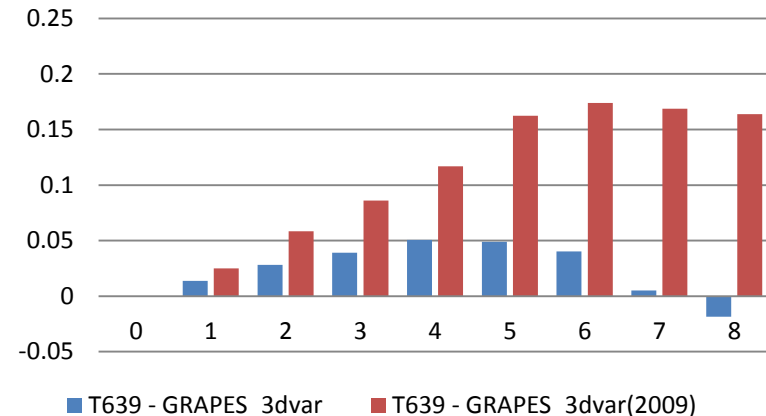


GRAPES-GFS已经接近T639的能力

北半球 T639 - GRAPES



东亚 T639 - GRAPES



GRAPES面向未来发展的瓶颈问题

toward massively parallel computer architectures with $O(10^4+)$ cores

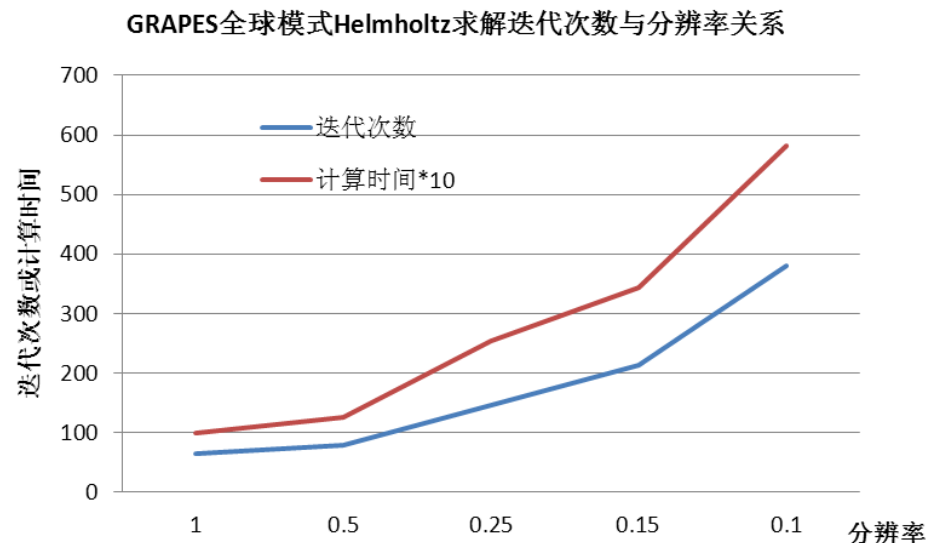
- 模式方程组

- 守恒性问题
 - 浅层大气近似问题

~10km全球
~1km中尺度

- 精度、效率、可扩展性

- Singular nature of the regular LAT/LON grids
 - Lost grid locality for finding departure point
 - Implicit numerics
 - Helmholtz equation
 - Semi-Lagrangian scheme
 - I/O

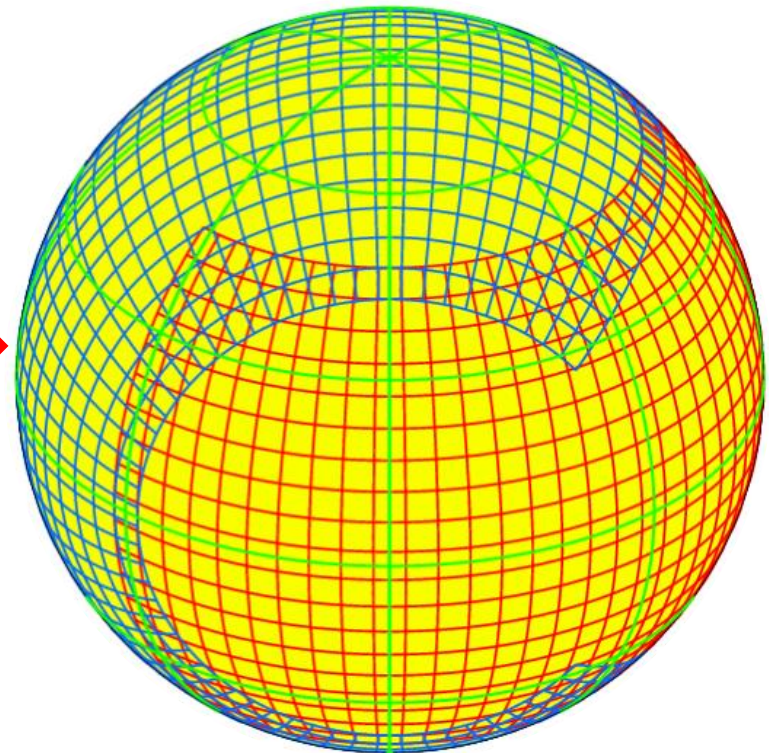
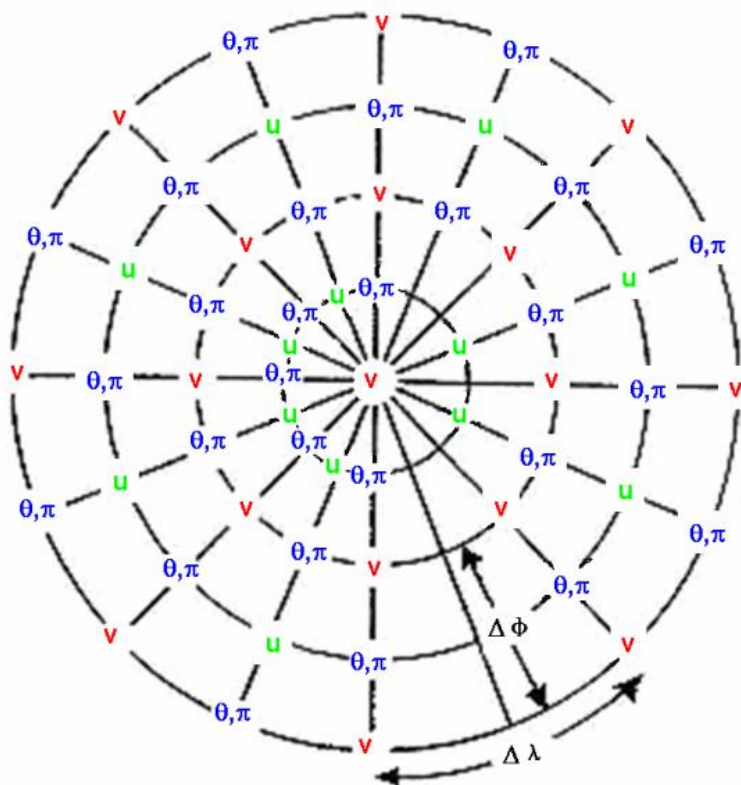


For the future development, we need to recall:

- scales well on hundreds of thousands of processors
- resolves well the energy spectrum at all scales
- **Equation set**
 - **Non-conservative form** using Exner pressure, momentum and potential temperature, e.g., **current GRAPES**
 - **Conservative form** using density, momentum and potential temperature, e.g., **after removing weakness from current GRAPES**
 - **Conservative form** using density, momentum and total energy, **attractive for high resolution, non-hydrostatic flow** → naturally accounts for the dissipative conversion of potential and kinetic energy into internal energy
- **Quasi-uniform grids** → remove LAT/LON singularity
- **Advection scheme:** Eulerian vs. semi-Lagrangian
- **Temporal discretization:** Explicit vs. implicit
- **Spatial discretization:** FD, FV, DG, SE, MCV



Option-1: GRAPES + Yinyang grid



Regular LAT/LON

Option-2: Next generation GRAPES model

New dynamic core

Based on multi-moment constrained finite volume method

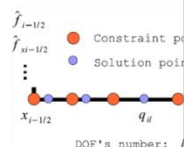
Multi-moment constrained finite volume method

Definition of multi-moments: the line-integrated average value (LIA moment), the point value (PV moment) and the derivative value (DV moment)

$$\bar{q}^{(x)}(t) \equiv \frac{1}{\Delta x_i} \int_{\delta x} q(x, t) dx,$$

$$q_{cp}(t) \equiv q(x_{cp}, t),$$

$$\partial_x^k q_{cp}(t) \equiv \frac{\partial^k}{\partial x^k} q(x_{cp}, t); \text{ with } k = 1, 2, \dots$$



Reconstruction:

A Lagrange interpolation polynomial of degree (L-1) is constructed as

$$\Psi(\phi : x) = \sum_{l=1}^L (\mathcal{B}_l \phi_l)$$

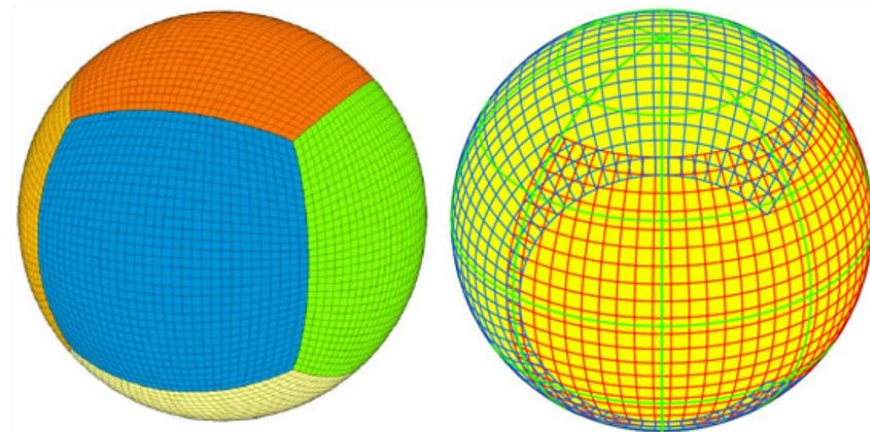
$$\text{where } \mathcal{B}_l = \prod_{p=1, p \neq l}^L \frac{(x - x_p)}{(x_l - x_p)}$$

DOFs and multi-moment constraints are the reconstruction polynomial

$$\begin{bmatrix} \phi_{i1} \\ \phi_{i2} \\ \vdots \\ \vdots \\ \phi_{iL} \end{bmatrix} = M \begin{bmatrix} \bar{\phi}_i^{(x)} \\ \phi_{icp} \\ \vdots \\ (\partial_x \phi)_n \\ \vdots \end{bmatrix}$$

- X. L. Li, C. G. Chen, X. S. Shen and F. Xiao, 2012: A multi-moment constrained non-hydrostatic atmospheric dynamics, Mon. Wea. Rev., in revision.
- Li, X. L., X. S. Shen, X. D. Peng, F. Xiao, Z. R. Zhuang, and C. G. Chen, 2012: F on yin-yang grid by multi-moment constrained finite volume scheme, Procedia C 1004-1013.

MCV (3rd and 4th order) + cubed grid or Yin-Yang grid

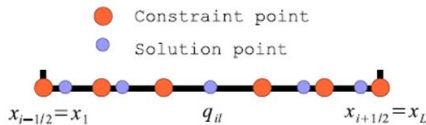


Further researches will be continued to develop 3D dynamical cores using the same methodology based on the popular structured spherical grids, such as structured cubed grid, Yin-Yang grid.

下一代模式的探索性研究

多矩约束有限体积(MCV)方法

(nodal type)



For conservation law

$$\frac{\partial q}{\partial t} + \frac{\partial f(q)}{\partial x} = 0$$

Multi-moment: the line-integrated average value (LIA moment),
value (PV moment) and the derivative value (DV moment)

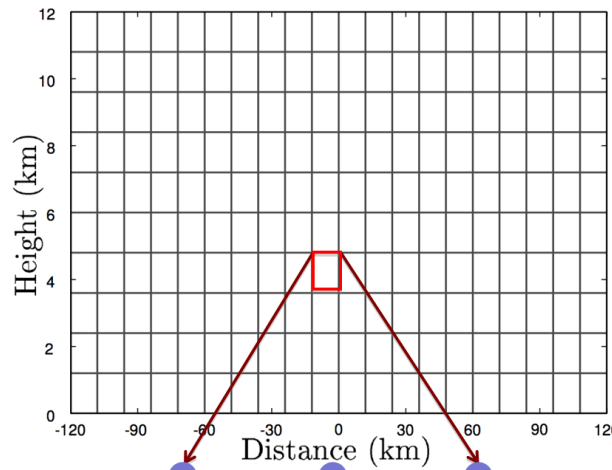
$$\bar{q}^{(x)}(t) \equiv \frac{1}{\Delta x_i} \int_{\delta x} q(x, t) dx,$$

$$q_{cp}(t) \equiv q(x_{cp}, t),$$

$$\partial_x^k q_{cp}(t) \equiv \frac{\partial^k}{\partial x^k} q(x_{cp}, t); \text{ with } k = 1, 2,$$

where $\Delta x_i = x_{i+1/2} - x_{i-1/2}$ and x_{cp} represents a constraint point within or at the boundary $x_1 \rightarrow x_L$ where constraints in terms of multi-moments are imposed. **The constraint points coincide with the solution points.** The solution points (the unknowns, or the degrees of freedom) are more flexibly chosen in an MCV scheme, **not limited to the Gauss points or Gauss-Lobatto points.**

与传统有限体积方法区别和特点



网格单元定义自由度

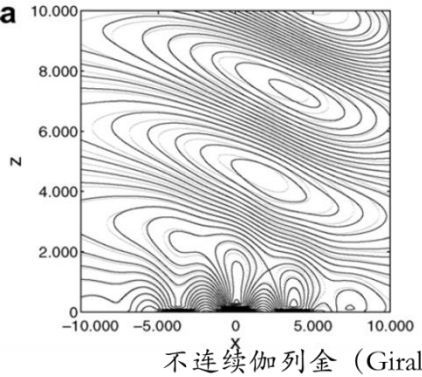
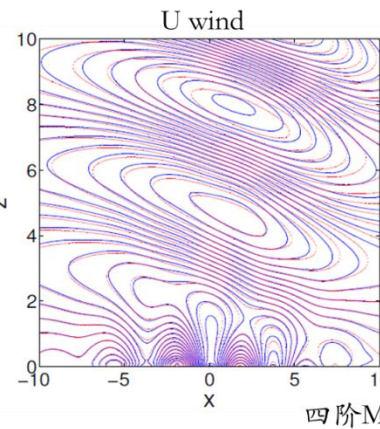
模式计算域

优势:

- 1) 局地高阶重构, 精度高
- 2) 局地计算量大、通信少, 故并行效率高
- 3) nodal类型, 易于源项处理, 坐标变换

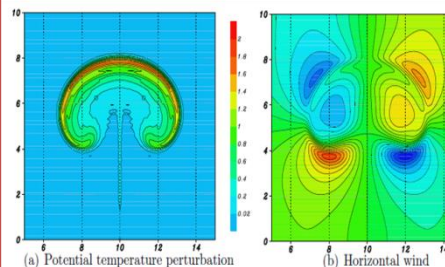
非静力完全可压缩多矩约束模式标准算例测试

- (1) 热泡试验
- (2) 密度流试验
- (3) 惯性重力波试验
- (4) 地形数值试验
 - (a) 线性静力山脉波
 - (b) 线性非静力山脉波
 - (c) Simple flow—A3 case
 - (d) Simple flow—A4 case
 - (e) 非线性山脉波—D1 case
 - (f) 非线性山脉波—D2 case
 - (g) Schar山脉波

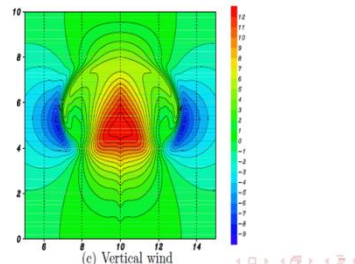
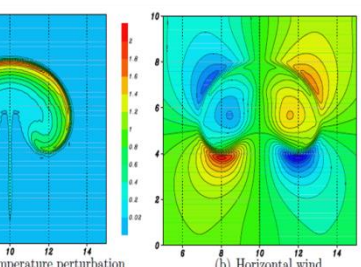


热泡试验

三阶MCV数值结果



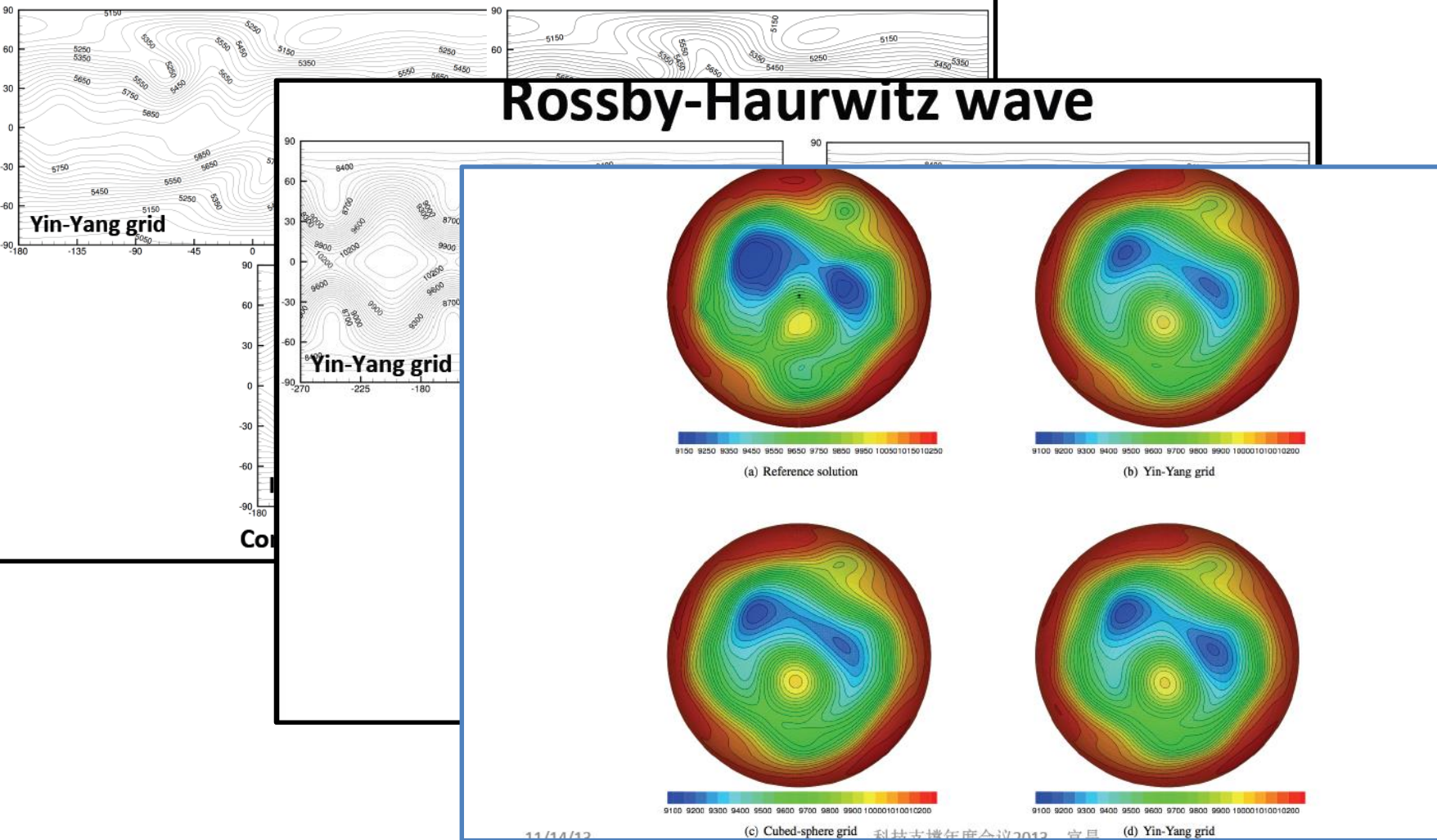
四阶MCV数值结果

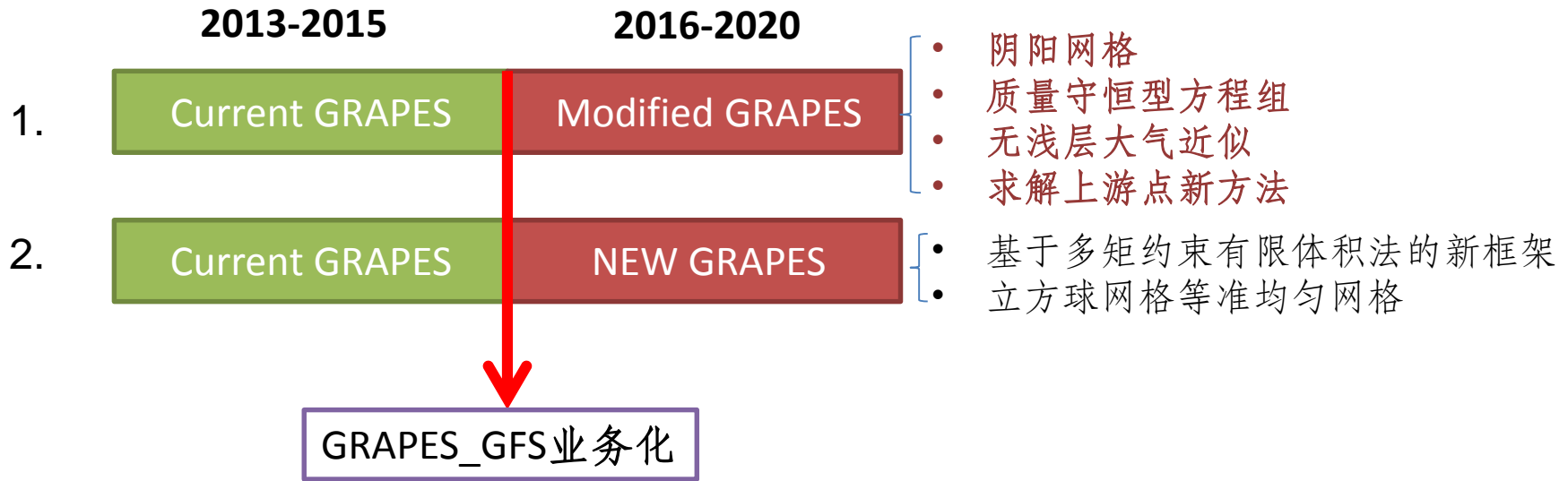


积分1000s数值结果

MCV浅水波模式理想试验

Zonal flow over isolated mountain





THANK YOU



High order Multi-moment Constrained finite Volume (MCV) method (Li and Xiao, JCP, 2009)

We define the moments *within single cell*, i.e. the cell-averaged value, the point-wise value and the derivatives of the field variable

$$\bar{q}_m^{(x)}(t) \equiv \frac{1}{\Delta x_i} \int_{\delta x} q_m(x, t) dx,$$

$$\partial_x^k q_{cpm}(t) \equiv \frac{\partial^k}{\partial x^k} q(x_{cpm}, t); \text{ with } k = 0, 1, \dots$$

Constraint conditions:

$$\frac{d}{dt}[\bar{q}_m^{(x)}(t)] = -\frac{1}{\Delta x_i} (\hat{f}_{Lm} - \hat{f}_{1m})$$

$$\frac{d}{dt}[q_{1m}(t)] = -\partial_x \hat{f}_{1m} \text{ and } \frac{d}{dt}[q_{Lm}(t)] = -\partial_x \hat{f}_{Lm}$$

$$\partial_t(q_x)_{cm}(t) = -\partial_x^2 \hat{f}_{cm},$$

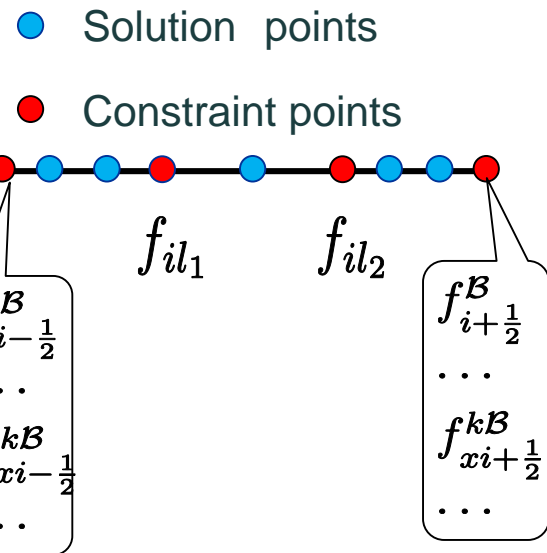
Approximate Riemann solvers

$$f_{xip}^{k\mathcal{B}} = \frac{1}{2} (f_{xip}^{k-} + f_{xip}^{k+} - R_{ip} |\Lambda_{ip}| R_{ip}^{-1} (q_{xip}^{k+} - q_{xip}^{k-}))$$

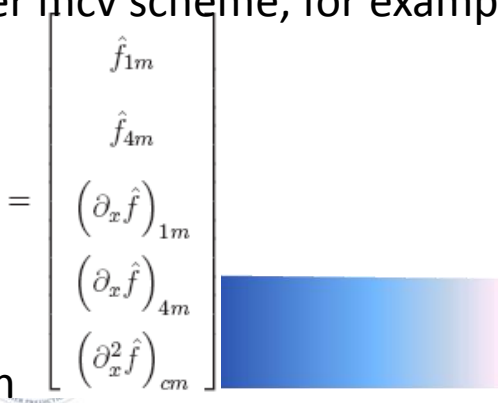
The unknowns (solution points) are updated in a fourth order mcv scheme, for example,

$$\begin{bmatrix} \frac{d}{dt}(q_{1m}) \\ \frac{d}{dt}(q_{2m}) \\ \frac{d}{dt}(q_{3m}) \\ \frac{d}{dt}(q_{4m}) \end{bmatrix} = \mathbf{M}_4^{(x)} \mathbf{F}_4^{(x)}$$

$$\mathbf{M}_4^{(x)} = \begin{bmatrix} 0 & 0 & -1 & 0 & 0 \\ \frac{4}{3\Delta x_i} & -\frac{4}{3\Delta x_i} & \frac{4}{27} & \frac{5}{27} & \frac{4\Delta x_i}{27} \\ \frac{4}{3\Delta x_i} & -\frac{4}{3\Delta x_i} & \frac{4}{27} & \frac{5}{27} & -\frac{4\Delta x_i}{27} \\ 0 & 0 & 0 & -1 & 0 \end{bmatrix}$$



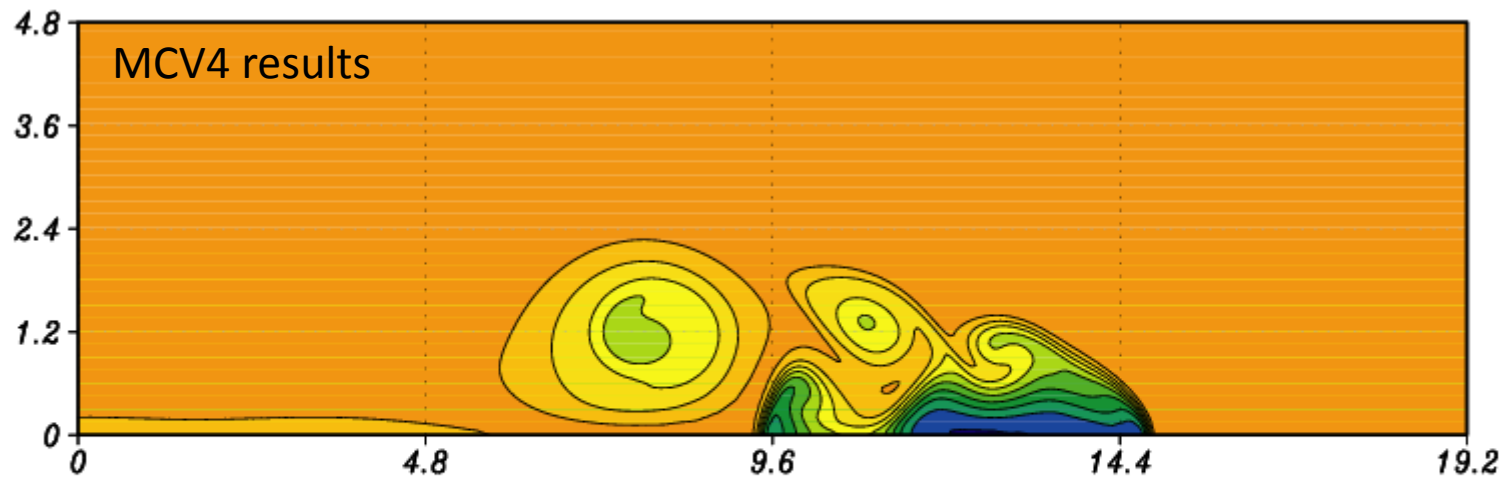
The same in multi-dimension, for example, y direction

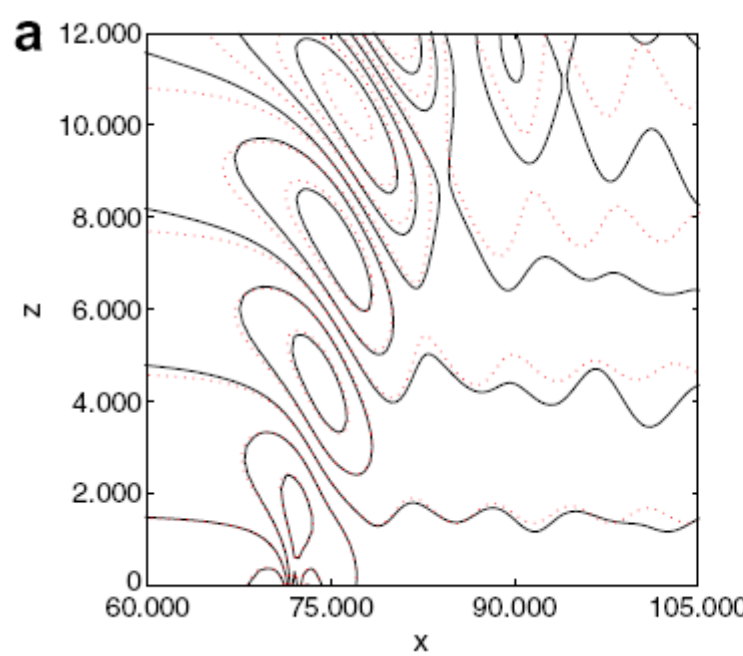


A nonhydrostatic atmospheric governing equation sets in the Cartesian system

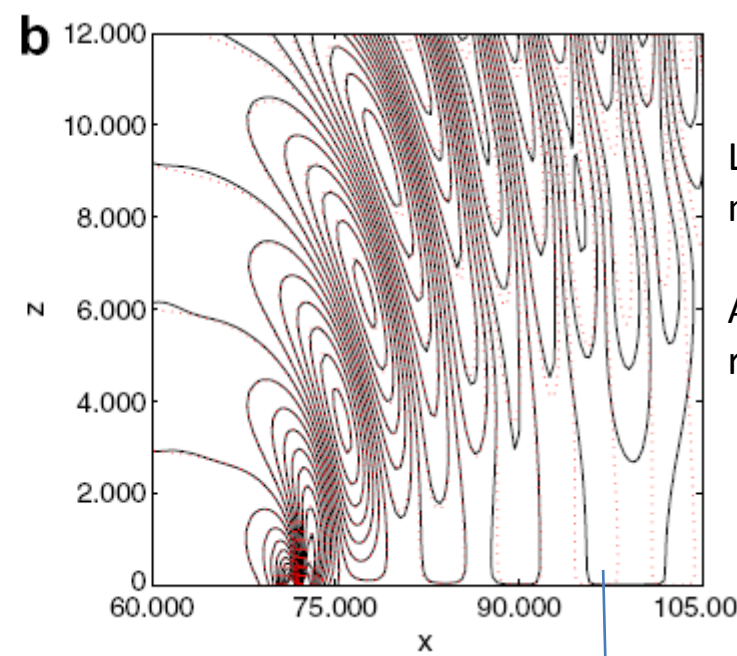
$$\frac{\partial \rho'}{\partial t} + \frac{1}{\sqrt{G}} \frac{\partial}{\partial \tilde{x}^j} \left(\sqrt{G} \rho \tilde{u}^j \right) = 0 \quad \rho(\mathbf{x}, t) = \bar{\rho}(\mathbf{x}) + \rho'(\mathbf{x}, t)$$
$$\frac{\partial \rho u}{\partial t} + \frac{1}{\sqrt{G}} \left(\frac{\partial}{\partial \tilde{x}^j} \left(\sqrt{G} \rho u \tilde{u}^j \right) + \frac{\partial}{\partial \tilde{x}^j} \left(\sqrt{G} G^{1j} p' \right) \right) = 0 \quad p(\mathbf{x}, t) = \bar{p}(\mathbf{x}) + p'(\mathbf{x}, t)$$
$$\frac{\partial \rho w}{\partial t} + \frac{1}{\sqrt{G}} \left(\frac{\partial}{\partial \tilde{x}^j} \left(\sqrt{G} \rho w \tilde{u}^j \right) + \frac{\partial p'}{\partial \tilde{x}^3} \right) = -\rho' g \quad (\rho\theta)(\mathbf{x}, t) = \overline{(\rho\theta)}(\mathbf{x}) + (\rho\theta)'(\mathbf{x}, t)$$
$$\frac{\partial(\rho\theta)'}{\partial t} + \frac{1}{\sqrt{G}} \frac{\partial}{\partial \tilde{x}^j} \left(\sqrt{G} \rho \theta \tilde{u}^j \right) = 0$$

Height-based terrain-following vertical coordinate (Gal-chen & Somerville 1975) is used. \sqrt{G} is transformation Jacobian.

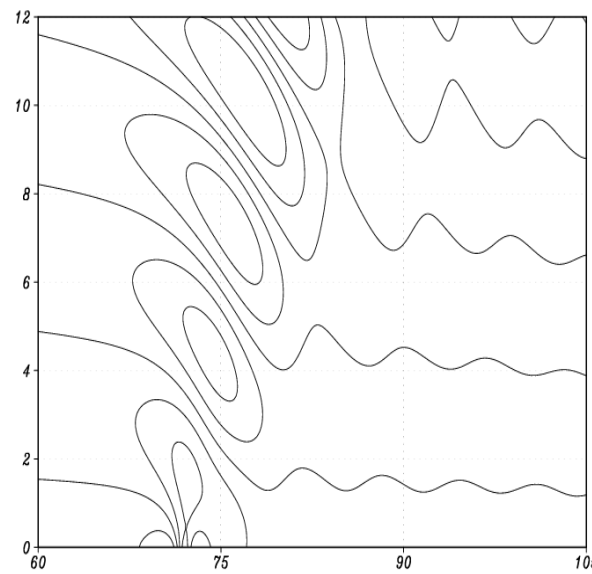




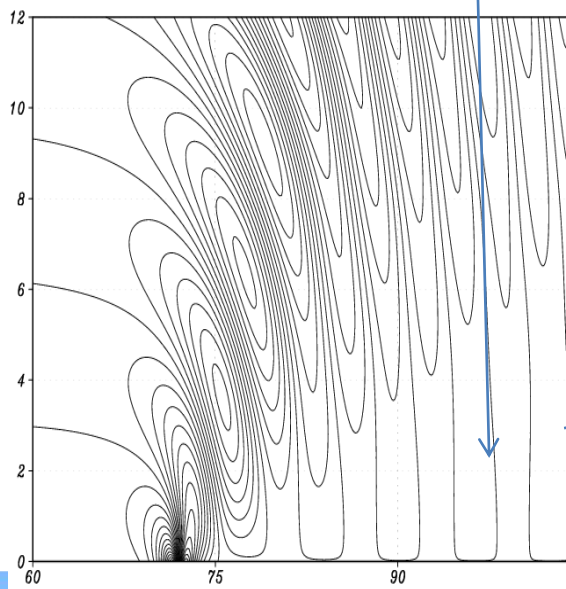
Discontinuous Galerkin results (Giraldo & Restelli, JCP, 2008)



Linear nonhydrostatic
mountain case
Analytic solution:
red dash line



Fourth order MCV results



zero contours